MINISTRY OF EDUCATION

THE ANNALS OF “DUNAREA DE JOS” UNIVERSITY OF GALATI

Fascicle IX
METALLURGY AND MATERIALS SCIENCE

YEAR XLI (XLVI)
March 2023, no. 1

ISSN 2668-4748; e-ISSN 2668-4756

2023
GALATI UNIVERSITY PRESS

THE ANNALS OF "DUNAREA DE JOS" UNIVERSITY OF GALATI
FASCICLE IX. METALLURGY AND MATERIALS SCIENCE
N°. 1 - 2023, ISSN 2668-4748; e-ISSN 2668-4756
Volume DOI: https://doi.org/10.35219/mms.2023.1

Table of Contents

THE ANNALS OF “DUNAREA DE JOS” UNIVERSITY OF GALATI
FASCICLE IX. METALLURGY AND MATERIALS SCIENCE
N^{o}. 1 - 2023, ISSN 2668-4748; e-ISSN 2668-4756
Article DOI: https://doi.org/10.35219/mms.2023.1.01

FIXINGS THAT ENSURE THE FREE MOVEMENT OF THE STRUCTURE FOR RESISTANCE IN RELATION TO NON-STRUCTURAL WALLS

Răzvan Andrei IERNUTAN, Luminița Monica PLEȘA
Technical University of Cluj-Napoca, Faculty of Civil Engineering, Romania
e-mail: razvan.ierntan@ccm.utcluj.ro; luminita.molnar@ccm.utcluj.ro

ABSTRACT

Recent earthquakes have confirmed that non-structural walls interacting mainly with frame structures are severely damaged during seismic actions endangering human lives. The ongoing life after earthquakes and major costs for rebuilding are deeply affected. In order to avoid this kind of drawbacks, the present paper suggests the introduction of a set of joints between the structure and the non-structural closing and division walls. The joints should observe the following: joints will be designed to provide free development of displacements in the plane of the walls with no major interactions in the structure; joints will be designed to provide transmission of the seismic forces acting perpendicularly to the non-structural walls towards the main structure. This paper will include several conclusions concerning the admission, constraint or removal of interactions between the structure and the closing and division walls.

KEYWORDS: fixing, free movement, masonry, non-structural walls

1. Introduction

Seismic performance requirements concern safety and diminishing of damage, in tight correlation with the ultimate service states (SLS) and ultimate limit states (ULS) [1, 2].

In general, no control is possible regarding the interaction between the frame and a masonry wall. Considering this lack of certitude, it is believed that the best solution consists in removing the masonry walls from the frame core and allowing it to move freely.

2. Calculation on non-structural walls subjected to perpendicular seismic loads on the wall plane

2.1. General aspects

To calculate the bending moments M_{EXd1} and M_{EXd2} under the action of uniform seismic loads, the non-structural walls (CNS) are modelled as elastic slabs placed down on the floor, then on the top, and laterally on the joints designed.

In the case of void panels, it will be applied 6.4.1 from CR-6-2013 [4, 5].

The bending moments M_{Rxd1} and M_{Rxd2} are calculated for a wall strip of width equal to 1.00 m and of thickness t.

$$M_{Rxd1} = w_w f_{xd1} \quad M_{Rxd2} = w_w f_{xd2}$$

where: f_{xd1} and f_{xd2} - represent the design bending tensile strengths perpendicular to the masonry plane.

$$w_w = 1000\, t^2 / 6$$

The requirement for stability is satisfied if:

$$M_{Rxd1} \geq M_{EXd1}$$
$$M_{Rxd2} \geq M_{EXd2}$$

If the strength requirement is not met, we can apply one of the solutions below.

In walls made with nut and feeder vertical joining, the wall is reinforced in the horizontal joints.

In the other cases, the dimensions of the walls are reduced by belts and middle piles so that the formed masonry panels respect the strength requirement.

The piles and the belts will be dimensioned to take over the stresses coming from the loads

Nº. 1 - 2023, ISSN 2668-4748; e-ISSN 2668-4756
Article DOI: https://doi.org/10.35219/mms.2023.1.01

perpendicular to the unstructural masonry and to be transmitted to the main structure through the loads.

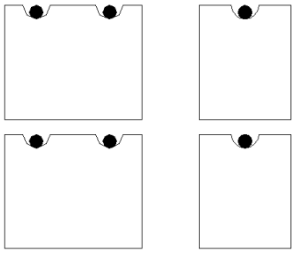

Fig. 1. *Reinforcement of masonry in horizontal joint*

In the case of larger size masonry members, such as firewalls, gables, lunettes, etc. acting in cantilevers, CR-6-2013 provisions will be followed. [4, 5].

2.2. Types of joints

2.1.1. Joint in a structure

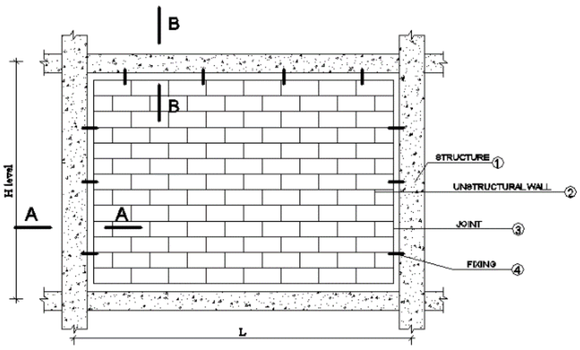

Fig. 2. *Masonry joints of vertical and horizontal elements*

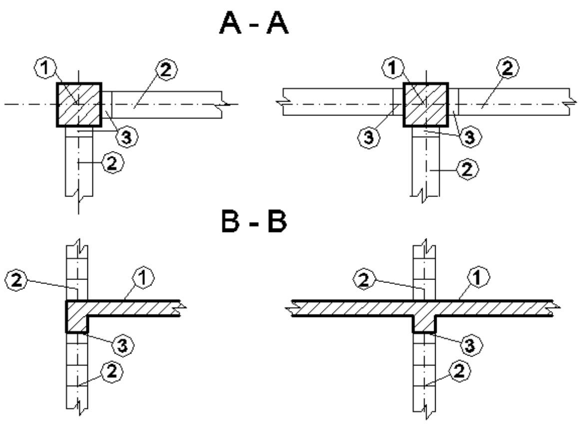

Fig. 3. *Detail A-A. Detail B-B*

Joints of vertical elements made from reinforced concrete (piles, membranes).

2.1.2. Fixing with steel bars

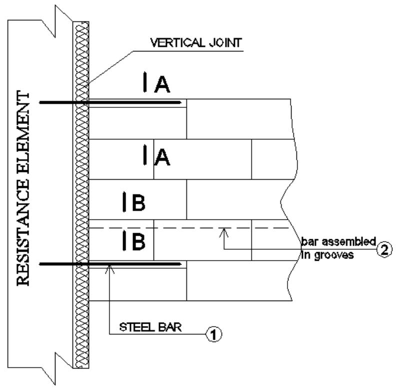

Fig. 4. *Section A-A*

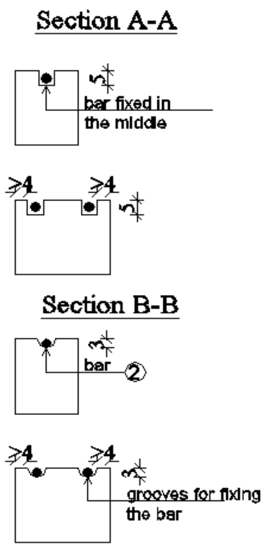

Fig. 5. *Detail A-A, Detail B-B*

The diameter of the bars 1, their number and the distance between the bars will be established by calculation.

Bars are fixed in the structural member by making a hole in the formwork before the member is cast or by making a hole in the concrete block and joining it with resins or cement mortars [3].

The slot made in the concrete block can be filled with elastic materials.

Bars 2 (if necessary) are mounted in grooves and fixed with minimum M5 mortar, (section B-B) [1, 2, 6].

THE ANNALS OF “DUNAREA DE JOS” UNIVERSITY OF GALATI
FASCICLE IX. METALLURGY AND MATERIALS SCIENCE
Nº. 1 - 2023, ISSN 2668-4748; e-ISSN 2668-4756
Article DOI: https://doi.org/10.35219/mms.2023.1.01

2.3. Metal strip joints with vertical strength members

2.1.3. Simple fixing

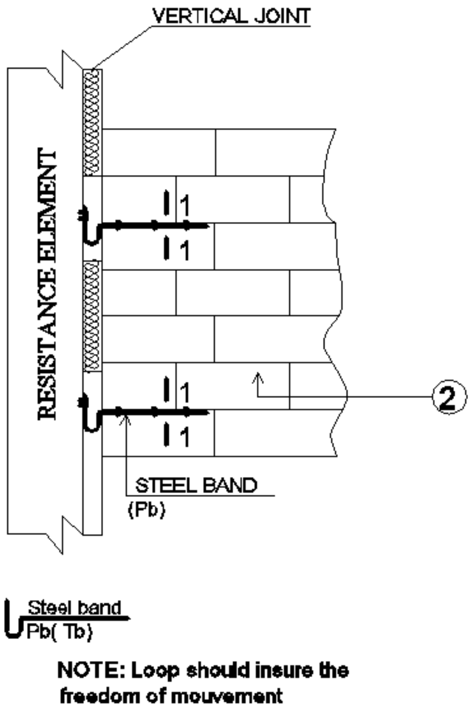

Fig. 6. *Simple fixing*

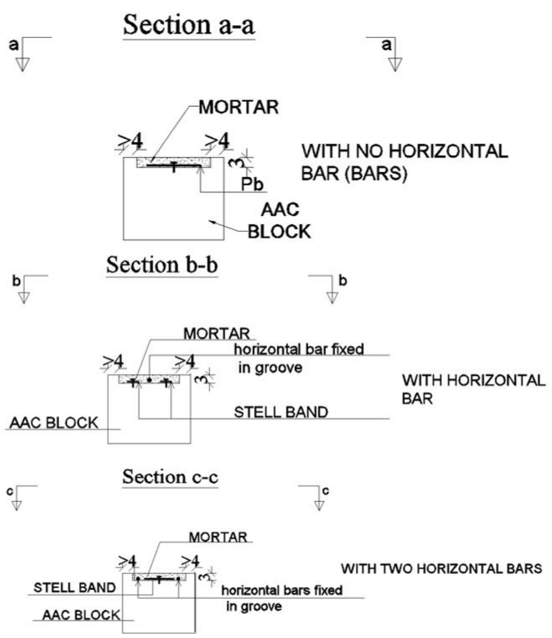

Fig. 7. *Sections a-a; b-b and c-c*

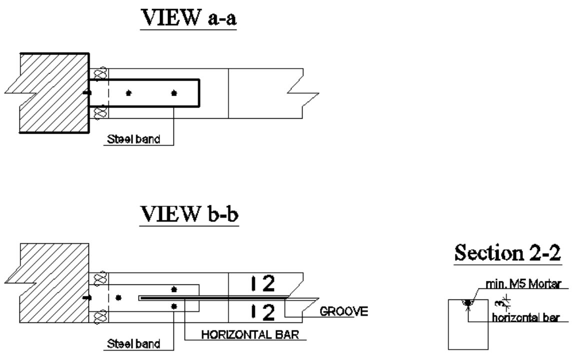

Fig. 8. *Section 1-1*

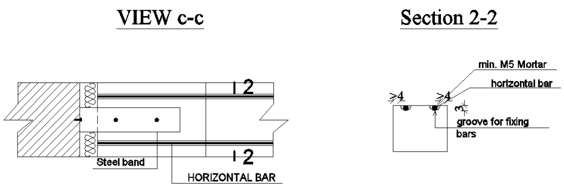

Fig. 9. *Double joint*

2.1.4. Double joint

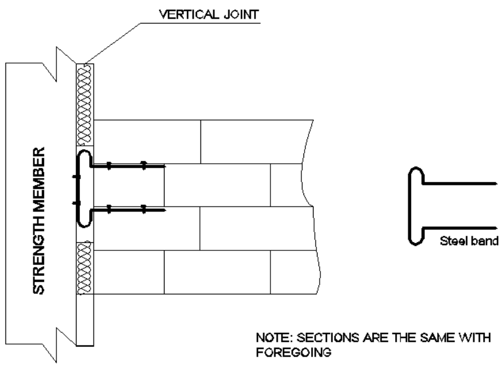

Fig. 10. *Fixing with steel band*

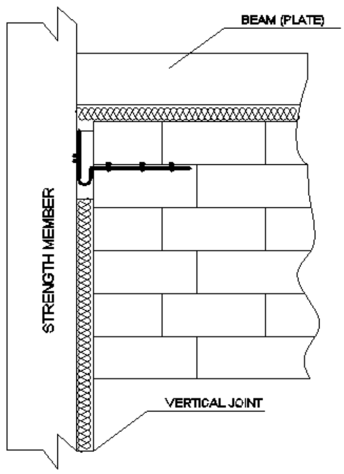

Fig. 11. *Simple joint*

Nº. 1 - 2023, ISSN 2668-4748; e-ISSN 2668-4756
Article DOI: https://doi.org/10.35219/mms.2023.1.01

In vertical metal strength members, the same type of joints can be used, on condition that the joint is connected to the vertical metal member by welding, threaded screws or similar means.

2.1.5. Special joints

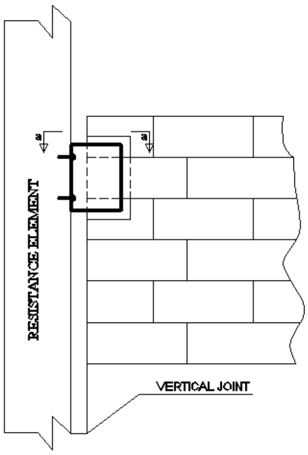

Fig. 12. Fixing with special pieces

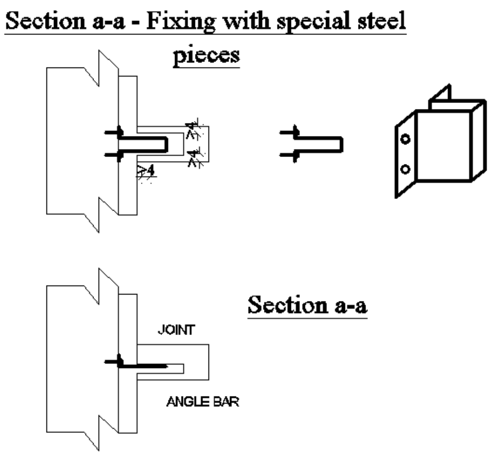

Fig. 13. Section a-a for fixing with special pieces

3. Wall top joining to beams or reinforced concrete slabs

3.1. Fixing with lateral angle bars

If it is necessary to have more blocks for taking over the normal to-the-wall horizontal loads, bars can be mounted in the grooves and fixed with mortars [3].

The angle bars will be inserted after the masonry is erected.

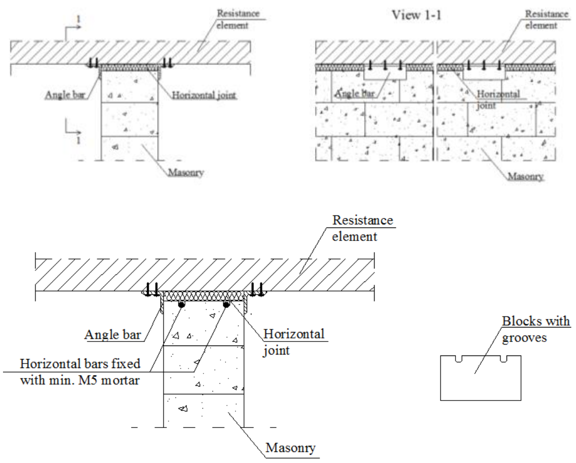

Fig. 14. Fixing with lateral angle bars

3.2. Fixing with angle bar incorporated in masonry

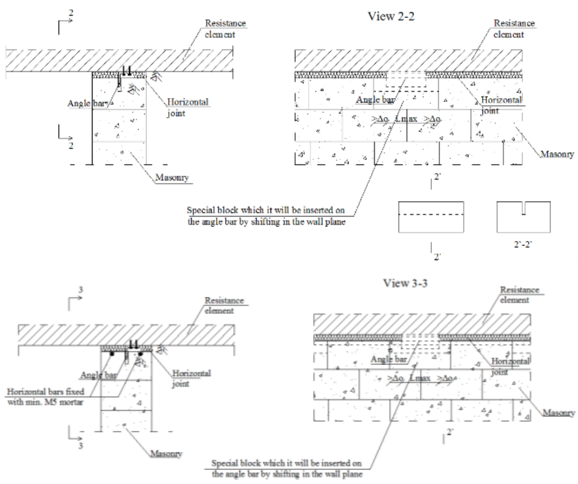

Fig. 15. Fixing with angle bar incorporated in masonry

To take over the horizontal loads of more BCA blocks, horizontal steel bars will be incorporated in the mortar.

4. Conclusions

It is appreciated that the interaction between the frame and the masonry panel (framed masonry) is an extremely complex issue, with many aspects still to be studied. In most cases, in the current design practice, this interaction is neglected (and this is recommended in the design codes), but the detriments of interaction cannot be eliminated and with severe earthquakes, they are always visible. We think that the solutions presented here are applicable and their use will lead to the desired consequence that is the joints will separate the masonry walls from the structure. In this way, the system will become a controllable system.

References

[1]. Răzvan Andrei Iernutan, Florin Babota, *Autoclaved Cellular Concrete (ACC) Masonry with Vertical Hollows Confined with Disperse Reinforced Concrete*, Procedia Engineering, vol. 181, p. 300-307, ISSN 1877-7058, 2017.

[2]. Razvan Andrei Iernutan, Florin Babota, Raluca Istoan, *Carbon fibre reinforced aluminium mesh composite materials*, Journal Procedia Manufacturing, vol. 32, p. 901-907, Elsevier, 2019.

[3]. Drobiec Ł., Radosław Jasiński, Tomasz Rybarczyk, *The influence of the type of mortar on the compressive behaviour of walls made of Autoclaved Aerated Concrete (AAC)*, Brick and Block Masonry–Trends, Innovations and Challenges, Taylor & Francis Group, London, p. 1531-1538, 2016.

[4]. ***, CR6–2013, *Codul de proiectare pentru structuri din zidărie (Code design for masonry structures)*.

[5]. ***, P100/1-2013, *Cod de proiectare seismică - Partea I: Prevederi de proiectare pentru constructii*.

[6]. Dorina Sucală, Sorina Anamaria Ciplea, Ilie Nicolae Sucală, *Management of historical building rehabilitation*, 6th edition of the RMEE International Management Conference: "Performance management or Management Performance", Cluj-Napoca, 20-22 of September, 2018.

THE ANNALS OF "DUNAREA DE JOS" UNIVERSITY OF GALATI
FASCICLE IX. METALLURGY AND MATERIALS SCIENCE
Nº. 1 - 2023, ISSN 2668-4748; e-ISSN 2668-4756
Article DOI: https://doi.org/10.35219/mms.2023.1.02

SUSTAINABILITY IN CONSTRUCTION

Simona STANCA
Technical University of Cluj-Napoca, Buildings and Management Department, Romania
e-mail: simona.stanca@ccm.utcluj.ro

ABSTRACT

The main theme of this work is the sustainability of buildings and their relevance for sustainable development in Romania and Europe in the current context of orientation towards sustainable augmentation, minimizing the negative impact on the environment.

A sustainable building must be designed to use the necessary resources: energy, water, and materials in a more efficient way while aiming at reducing the impact that the construction itself has on the health of the occupants but also on the environment.

As it is known, human activity in the last few centuries has led to the consumption of resources and the spread of pollutants in the environment.

According to statistics, over time it has been proven that the construction sector is one of the most active contemporary polluters. The largest amount of greenhouse gas emissions from the building sector results from the use of energy (e.g., for heating, lighting, etc.). Thus, it is demonstrated the need to decrease energy consumption for the use of buildings, but also for their construction and recycling.

KEYWORDS: building materials, natural resources, sustainable development

1. Introduction

Sustainability in construction refers to the design, construction, and maintenance of buildings and infrastructure in an environmentally responsible manner, with the goal of reducing their negative impact on the environment and preserving resources for future generations. This includes using energy-efficient materials and systems, reducing waste and emissions, preserving natural resources, and promoting healthy indoor environments.

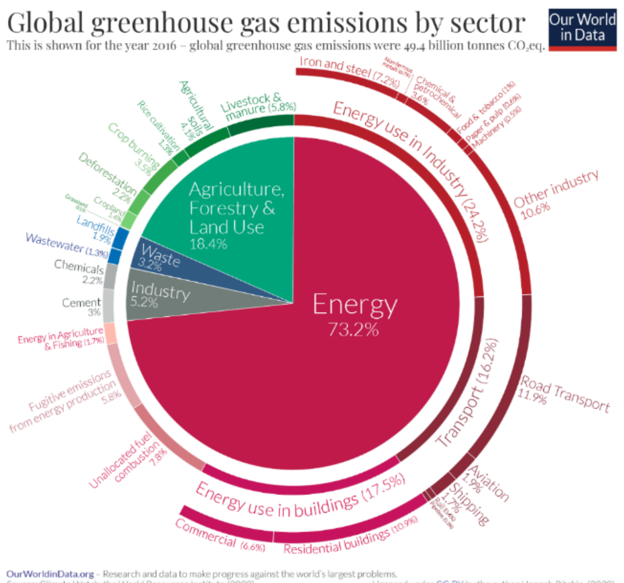

Fig. 1. Global greenhouse gas emission by sectors [11]

Nº. 1 - 2023, ISSN 2668-4748; e-ISSN 2668-4756
Article DOI: https://doi.org/10.35219/mms.2023.1.02

Sustainability in the construction sector is important both in terms of energy used in construction and in terms of CO_2 emissions (Fig. 1) [11].

Carbon dioxide emissions are the primary cause of global climate change and if humanity wants to avoid the most severe effects of it, we must reduce these emissions.

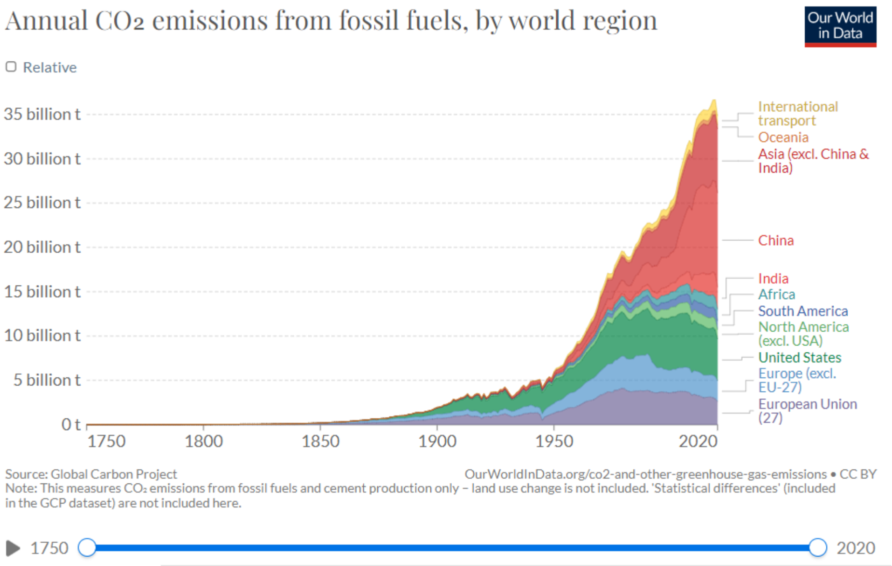

Fig. 2. *Annual CO_2 emissions from fossil fuels, by world region [12]*

In the twentieth century, Europe and the United States were responsible for the majority of global emissions, with over 90% of emissions coming from these two regions in 1900 and more than 85% in 1950 (Fig. 2) [12].

As we look to the future, it is critical to recognize the need to balance environmental and human welfare when considering CO_2 emissions, as both have a direct impact on the living conditions of generations to come. We must work together to develop a sustainable future that offers a high quality of life for everyone (Fig. 3) [13], (Fig. 4) [14].

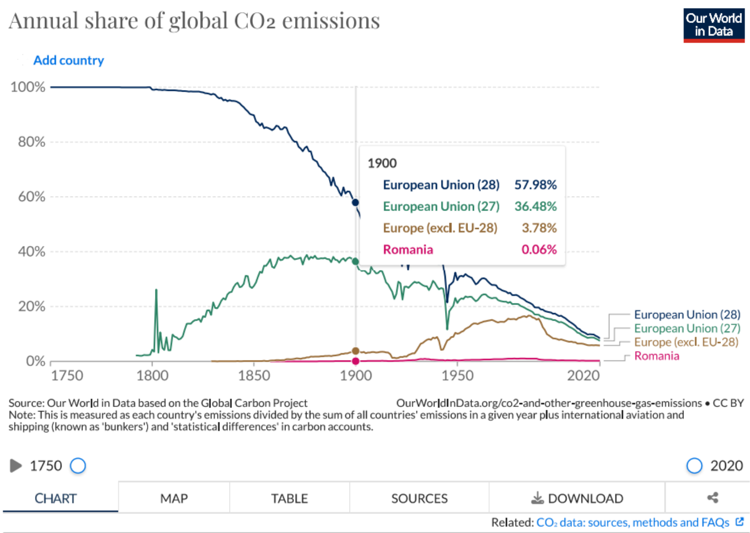

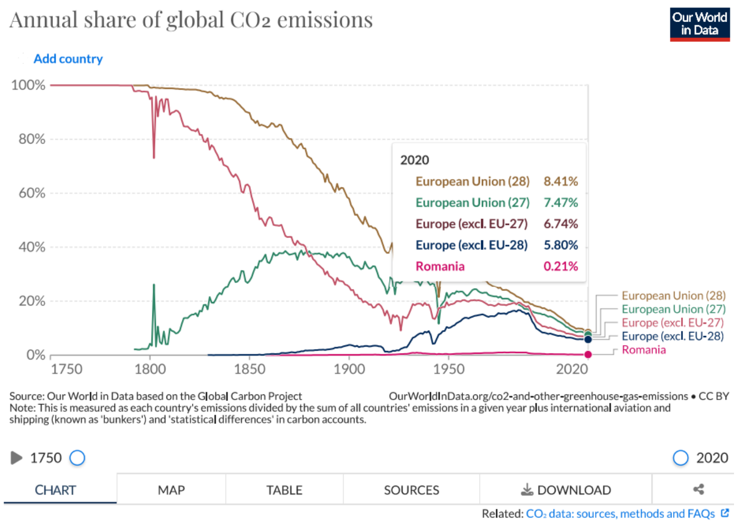

***Fig. 3.** The total amount of carbon dioxide released into the atmosphere in Europe each year, 1900/2020 [13]*

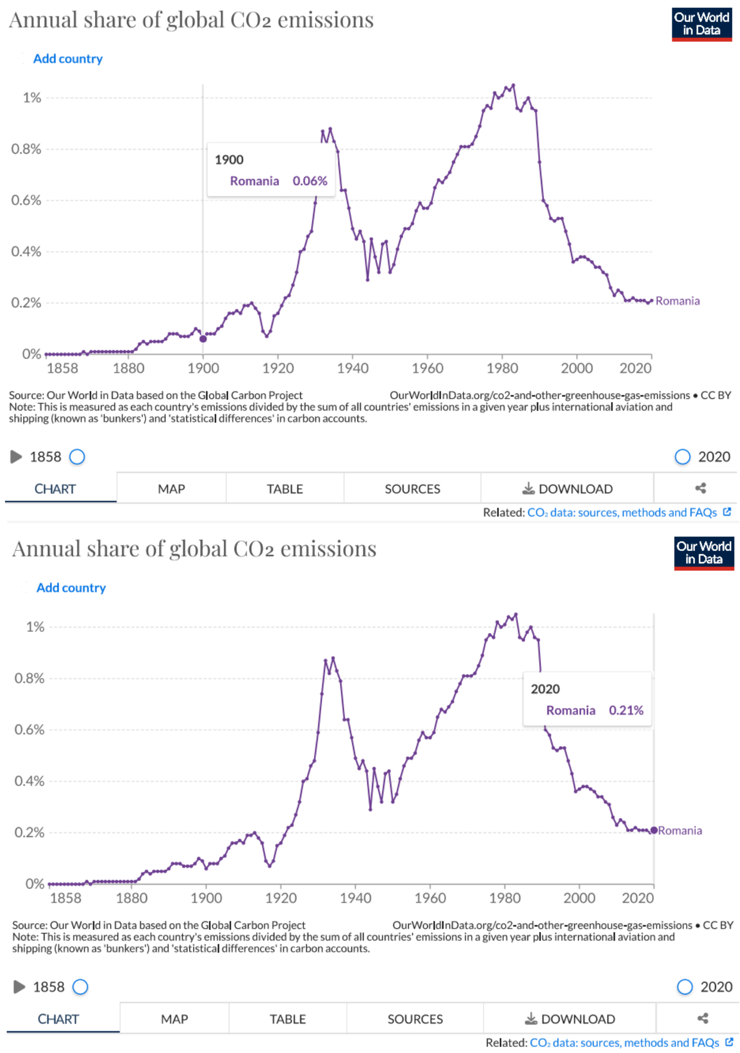

***Fig. 4.** The quantity of carbon dioxide released into the atmosphere in Romania over the course of a year, 1900/2020 [14]*

Nº. 1 - 2023, ISSN 2668-4748; e-ISSN 2668-4756
Article DOI: https://doi.org/10.35219/mms.2023.1.02

2. Sustainability in building development

The construction industry is one of the largest users of natural resources while being one of the most dynamic sectors worldwide [1].

Sustainability in the development of buildings refers to the implementation of measures that allow their sustainable execution, measures that ensure a long-term existence of the building, without affecting the environment and respecting economic principles.

Given the global scarcity of natural resources, the main challenge for producers and consumers is 'to achieve more by consuming fewer resources" [7].

Given the limited nature of these resources, the adoption of sustainable construction methods and the use of renewable and recyclable materials, as well as the reduction of energy consumption and waste, over time, will have a direct effect in reducing the impact on the environment while providing a healthier and more comfortable lifestyle [2].

Sustainability in the development of buildings is a vast and complex subject, which must be considered from the design stage because the potential impact on the environment is significant (Fig. 5) [4].

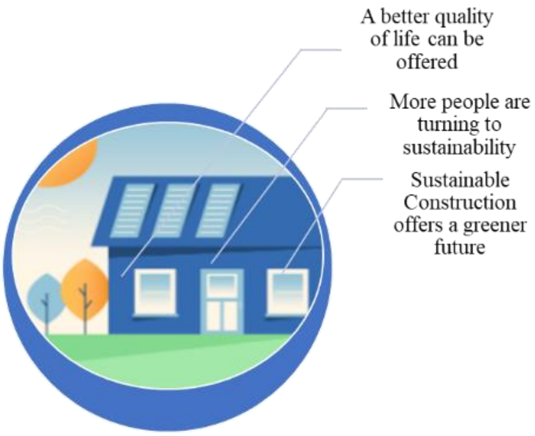

Fig. 5. *The importance of sustainability in construction*

Sustainable building incorporates the concept of creating a healthy environment with consideration for ecological principles. Professor Charles J. Kibert states that sustainable construction is based on six principles: conservation, reuse, recycling/renewal, nature protection, and the production of non-toxic and high-quality materials [4].

According to the European Commission, the construction sector produces about 1/3 of the total waste. As a global industry, it contributes 11% of greenhouse gas emissions, and its current volume of use of natural resources is unsustainable and substantially compromises the environment for the purpose of its development [16].

The aim is to reduce the environmental impact of the industry by using sustainable development practices, energy efficiency, and harnessing green technology.

Sustainable construction considers the use of resources (energy, natural resources), their impact on the environment, and specific risks to human safety [3].

The moderate use of locally available building materials and compliant, energy-efficient but also sustainable technologies have become a major topic of policymaking, research, and innovation at a global level [8].

3. Durable building materials

In order for construction to be considered sustainable, building materials should be chosen based on their ability to reduce the carbon footprint of a building and their durability. Durable materials should come from a local source, be recyclable, be produced in a sustainable way, and be made from materials that can be recycled. Using these criteria, materials such as concrete, steel, plastic, wood, and bricks can all be used in the construction of sustainable buildings [4, 5, 9].

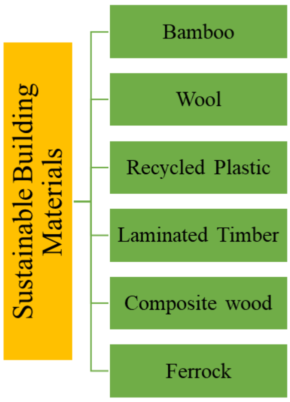

Fig. 6. *Sustainable building materials*

Types of durable building materials (Fig. 6) [9]:
- straw bale;
- wool;
- recycled steel;
- recycled plastic;
- beaten earth;
- processed wood (composite wood);
- bamboo, etc.

4. The advantages of using sustainable construction materials

Sustainable construction is not just about using the latest materials. It is also about the use of

THE ANNALS OF "DUNAREA DE JOS" UNIVERSITY OF GALATI
FASCICLE IX. METALLURGY AND MATERIALS SCIENCE
Nº. 1 - 2023, ISSN 2668-4748; e-ISSN 2668-4756
Article DOI: https://doi.org/10.35219/mms.2023.1.02

construction methods and technologies that increase renewable and sustainable efforts [2].

Advantages of using sustainable building materials (Fig. 7) [9]:

- waste reduction;
- low emissions;
- lower costs.

Fig. 7. *Benefits of sustainable materials*

As the dangers of climate change become more and more apparent, the need for sustainable construction grows. Despite the challenges that come along with it, sustainable construction has the potential to create a cleaner, greener future for us all. The demand for sustainable construction is rising, and the benefits it brings are becoming more and more evident. (Fig. 8) [10, 15], (Fig. 9) [6].

Fig. 8. *The benefits of sustainable construction [10, 15]*

Fig. 9. *Sustainable construction methods, benefits and challenge [6]*

5. Conclusions

The evolution of human society has always produced a major impact on the development of buildings, which constantly evolve with humanity, according to needs and requirements.

Given the current ecological context, climate change, and the high and growing consumption of non-renewable resources, it is important to find alternative, sustainable, renewable, recyclable, and efficient solutions in the construction field.

The ultimate goal of creating sustainable buildings is to reduce the negative impact of the built environment on both human health and the surroundings. This is done by improving energy efficiency, conserving natural resources, protecting occupants' health, and minimizing waste, pollution, and environmental degradation. To achieve this, new technologies are continually being developed to supplement existing practices.

References

[1]. Maier A., Molnar L. Monica, Stanca S., *Challenges regarding sustainable development from building materials perspective*, International Conference Interdisciplinarity in Engineering, 38th IBIMA Conference, Seville, Spain, ISBN: 978-0-9998551-7-1, 23-24 November 2021.

[2]. Stanca S., *Refurbishment of Decommissioned Buildings in the Context of Sustainable Development*, Bul. Inst. Polit. Iași, 62 (66), 1, p. 61-71, ISSN: 1224-3884 (p), ISSN: 2068-4762 (e), 2016.

[3]. ***, https://www.activesustainability.com/construction-and-urban-development/sustainable-building-materials/?_adin=01833301559, accessed on 2.11.2022.

[4]. ***, https://www.bigrentz.com/blog/sustainable-construction, accessed on 2.11.2022.

[5]. ***, https://www.bigrentz.com/blog/the-future-of-building-materials, accessed on 4.11.2022.

[6]. *****, https://engg.dypvp.edu.in/blogs/sustainable-construction-methods-benefits-and-challenges, accessed on 4.11.2022.
[7]. *****, https://www.europarl.europa.eu/factsheets/ro/sheet/77/consumul-si-productia-durabile, accessed on 5.11.2022.
[8]. *****, https://www.frontiersin.org/research-topics/33008/construction-materials-and-technologies-a-sustainable-approach, accessed on 12.11.2022.
[9]. *****, https://mtcopeland.com/blog/a-guide-to-sustainable-building-materials/, accessed on 14.11.2022.
[10]. *****, https://nestcon.com/sustainable-construction-methods-and-benefits/, accessed on 21.11.2022.
[11]. *****, https://ourworldindata.org/emissions-by-sector), accessed on 9.12.2022.
[12]. *****, https://ourworldindata.org/grapher/annual-co-emissions-by-region, accessed on 9.12.2022.
[13]. *****, https://ourworldindata.org/grapher/annual-share-of-co2-emissions?country=European+Union+%2827%29~ROU~Europe+%28excl.+EU-28%29~European+Union+%2828%29, accessed on 9.12.2022.
[14]. *****, https://ourworldindata.org/grapher/annual-share-of-co2-emissions?country=~ROU, accessed on 9.12.2022.
[15]. *****, https://www.renewablesinafrica.com/africas-increasing-investment-in-sustainable-construction/, accessed in 17.01.2023.
[16]. *****, https://www.rockwool.com/ro/despre-noi/filozofia-noastra/blog/importanta-sustenabilitatii-in-constructii/, accessed on 26.01.2023.

THE ANNALS OF "DUNAREA DE JOS" UNIVERSITY OF GALATI
FASCICLE IX. METALLURGY AND MATERIALS SCIENCE
N°. 1 - 2023, ISSN 2668-4748; e-ISSN 2668-4756
Article DOI: https://doi.org/10.35219/mms.2023.1.03

IMPORTANCE OF SIMULATING THE STEEL FLOW PROCESS IN THE TUNDISH, ON THE QUALITY OF CONTINUOUSLY CAST SLABS

Beatrice Daniela TUDOR, Ali Jawad Jaber MATROOD
"Dunarea de Jos" University of Galati, Romania
e-mail: beatrice.tudor@ugal.ro

ABSTRACT

The benefits of using mathematical modeling of the flow are obvious, the final objective being the elimination of as many inclusions as possible during the flow of steel through the tundish, and thus, obtaining steel with superior quality.

In this work, a simulation of the movement of the liquid alloy in the tundish was carried out, in order to highlight the erosion of its refractory lining. For this, we used SolidWorks, RealFlow, and ABAQUS programs.

Using these simulation programs, the filling method of the tundish, the contact area of the alloy jet with the tundish wall, and the "dead" areas are highlighted, as well as the turbulences that can appear during the flow, which have a negative impact on the quality of the steel.

KEYWORDS: tundish, simulation, mathematical modeling, steel quality

1. Introduction

The benefits of using mathematical modeling are obvious, and modeling has become much more accessible with the continuous evolution and availability of more powerful and faster computers.

Many quality problems that occur during continuous casting can be attributed to the control of fluid flow conditions.

The importance of the flow of liquid alloy starts from the manufacture of steel and from the refining operations, including in the pot.

The flow and filling of the tundish has as its objective, a chemical composition and a temperature as uniform and homogeneous as possible of the alloy, and the inclusions to be, as much as possible, removed in the slag layer. [1, 3].

The final objective remains the elimination of as many inclusions as possible, during the flow through the tundish, thus obtaining steel with superior quality.

The flow system must transport the molten steel, at the desired flow rate, from the pot to the tundish. The flow conditions should minimize contact with the atmosphere, avoid entrainment of slag or other exogenous inclusions, and help lift the inclusions in the slag. Achieving these objectives requires a study that takes into account all these phenomena that can influence the quality of the finished product, and requires a simulation of the flow, in order to reduce or eliminate them.

The tundish ensures a continuous flow of metal from the pot to the continuous casting machine. The flow in the tundish must ensure uniformity and the elimination of inclusions, while avoiding problems related to flow, such as turbulence, interruption, "dead" zones, etc. [2].

The flow can produce turbulence and can lead to the phenomenon of reoxidation, the entrainment of slag, and the time for the inclusions to be floated being insufficient. "Dead" zones are stagnant, colder regions that inhibit the removal of inclusions, and can contaminate the steel flowing through the tundish. If the liquid level is too low, high-velocity asymmetric flow can produce eddies, which can entrain surface slag [5].

The flow behavior in the tundish is influenced mainly by the size and shape of the tundish and by the location of flow control devices, such as dams. The flow pattern is also affected by the steel flow and its temperature distribution. Hotter steel tends to rise, having a lower density, while cooler steel tends to flow down the distributor walls. A temperature difference of only a few degrees is enough to completely reverse the flow direction.

The generation of inclusions and the impact on quality are the problems that arise during this operation of changing the casting pots. During this

THE ANNALS OF "DUNAREA DE JOS" UNIVERSITY OF GALATI
FASCICLE IX. METALLURGY AND MATERIALS SCIENCE
N°. 1 - 2023, ISSN 2668-4748; e-ISSN 2668-4756
Article DOI: https://doi.org/10.35219/mms.2023.1.03

operation, there is a period of temperature fluctuation and of the equilibrium state, which can lead to the reoxidation of the melt, the reactions with the casting slag, and the deposition of masonry particles from the pots. These aspects cause a negative impact on the steel quality in the tundish [4, 6].

2. Simulation of the liquid steel flow process in the tundish

The design of the distributor focused more on steady-state operation than on non-stationary state. Most new steel casting facilities use casting patterns and optimized flow control to improve inclusion removal. These larger tundishs provide the opportunity for an increased stationary time of the steel, and to pick up the inclusions into the slag, when using optimized flow control.

In order to better study and understand the processes that take place during the stationary and flow of the liquid alloy through the tundish, a simulation was made of the movement of the liquid alloy in the tundish, to highlight the erosion of its refractory lining [8].

It started from the creation of the 3D drawing of the tundish, beginning from the 2D drawing, which contains the real dimensions of the tundish. The drawing was made with the program SolidWorks, version 2016 Premium [7, 9].

The drawing has been exported in STL file format. The purpose of the STL file format was to convert the SolidWorks file.

The STL file was imported into MeshLab version 2022, in a 3D object file. The 3D object file was then opened in the RealFlow2015 software version. In Figure 1 you can see what the final drawing of the tundish looks like in the RealFlow software, starting from its drawing.

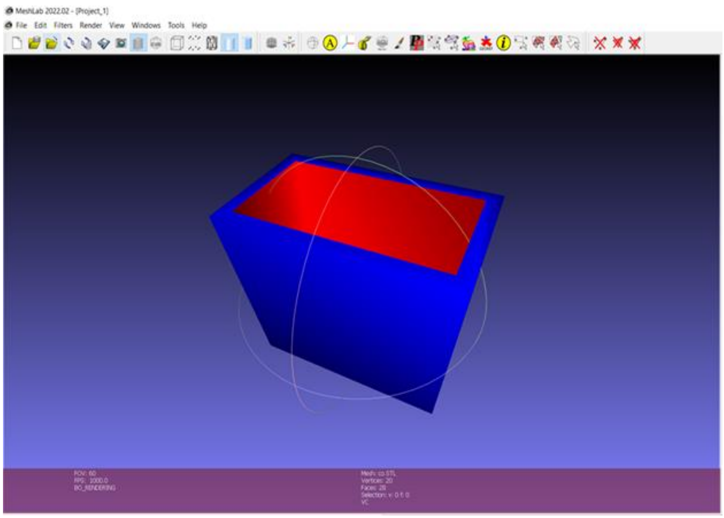

Fig. 1. *The drawing of the distributor from the continuous casting machine made in the Meshlab program*

The simulation of the flow of the liquid alloy in the tundish was done using the RealFlow program. RealFlow is a tool for simulating fluids in a dynamic system. The drawing made in Meshlab was converted into (a 3D object) format in the Realflow software (Fig. 2).

Through this simulation, it is possible to observe the filling mode of the tundish, with the first contact zone of the jet, with the wall of the tundish, with the "dead" areas, and the turbulences that may appear (Fig. 3).

The simulation of the flow of steel in the tundish, using this application (Realflow), has the purpose to highlight the flow of liquid steel, starting from the first impact of the jet with the wall made of ceramic material, until its complete filling. It is very clear, both the way of filling with the turbulences and "dead" areas, as well as the contact with the shotcrete wall. The movement and speed of the jet can tear the ceramic wall, degrading the liquid alloy, and can drive the inclusions inside the melt. The application of this simulation can help understand and combat these phenomena.

THE ANNALS OF “DUNAREA DE JOS” UNIVERSITY OF GALATI
FASCICLE IX. METALLURGY AND MATERIALS SCIENCE
N°. 1 - 2023, ISSN 2668-4748; e-ISSN 2668-4756
Article DOI: https://doi.org/10.35219/mms.2023.1.03

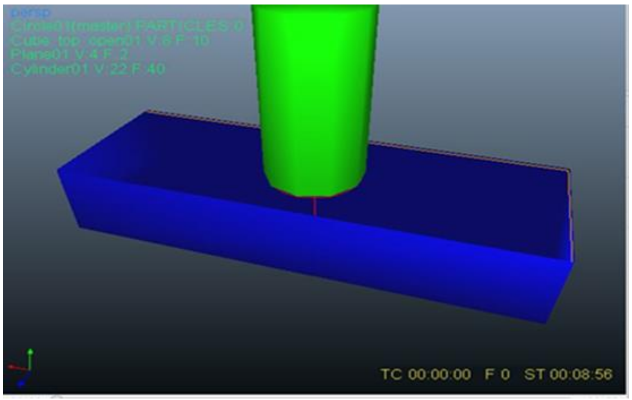

Fig. 2. *The drawing of the tundish, from the continuous casting machine, made in the Realflow program*

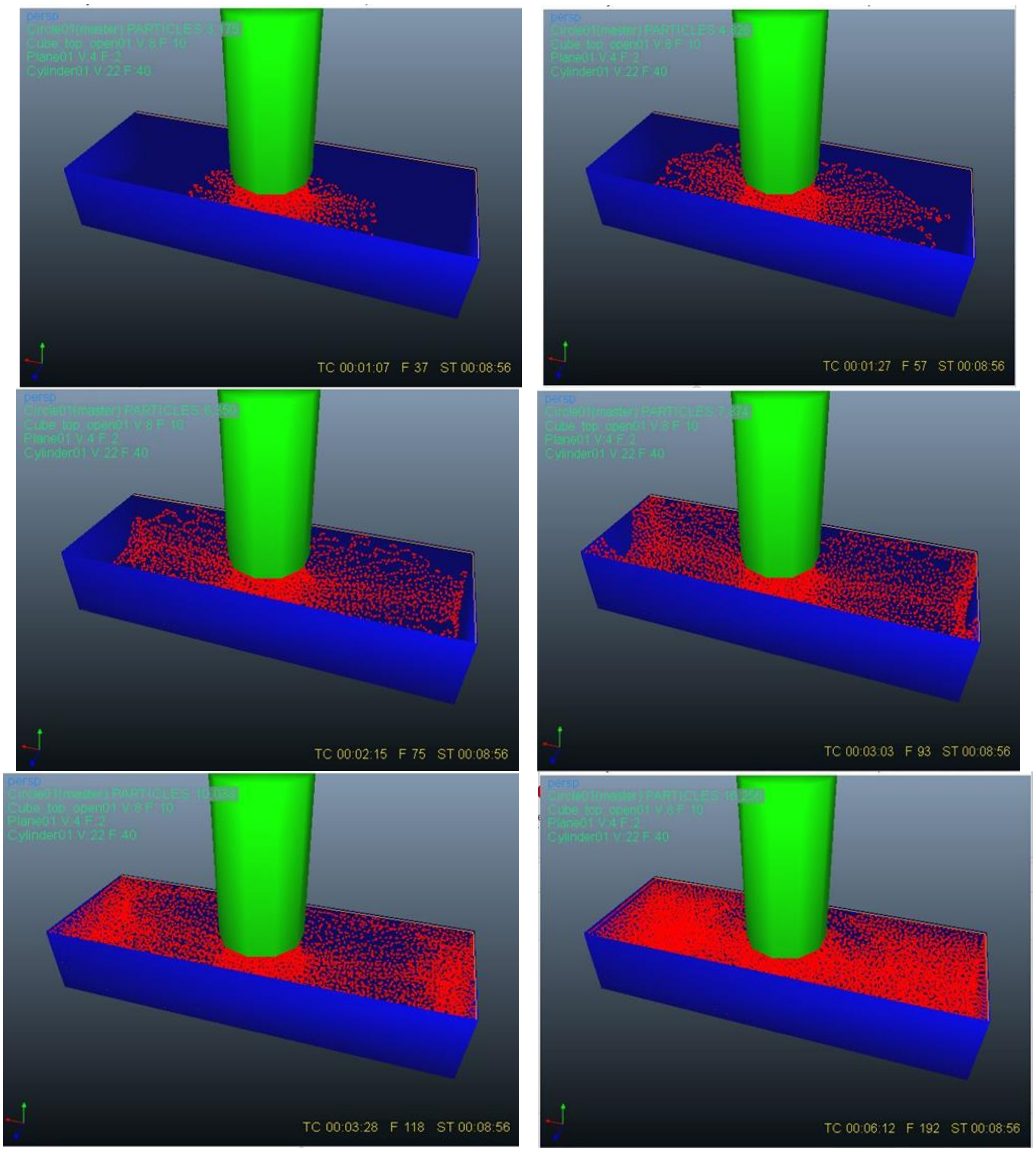

Fig. 3. *Captures from the development of the steel flow simulation program in the tundish*

THE ANNALS OF "DUNAREA DE JOS" UNIVERSITY OF GALATI
FASCICLE IX. METALLURGY AND MATERIALS SCIENCE
Nº. 1 - 2023, ISSN 2668-4748; e-ISSN 2668-4756
Article DOI: https://doi.org/10.35219/mms.2023.1.03

3. Simulating the compression resistance of the tundish walls

In order to better observe how the forces created by the liquid alloy act on the refractory lining of the tundish, the compression was simulated using the Solidworks and ABAQUS programs.

ABAQUS is a software suite for finite element analysis and computer-aided engineering of various materials subjected to mechanical tests [10, 11].

To study the compressive strength of the refractory concrete used to line the tundish, the ABAQUS program was applied, and a simulation was made of the compressive strength during filling with liquid alloy, on the walls of the tundish, made of refractory concrete. According to the data provided by the program, the force that develops on these walls, during filling, is 20 N. This is an important factor, which leads to the wear of the refractory lining (Fig. 4).

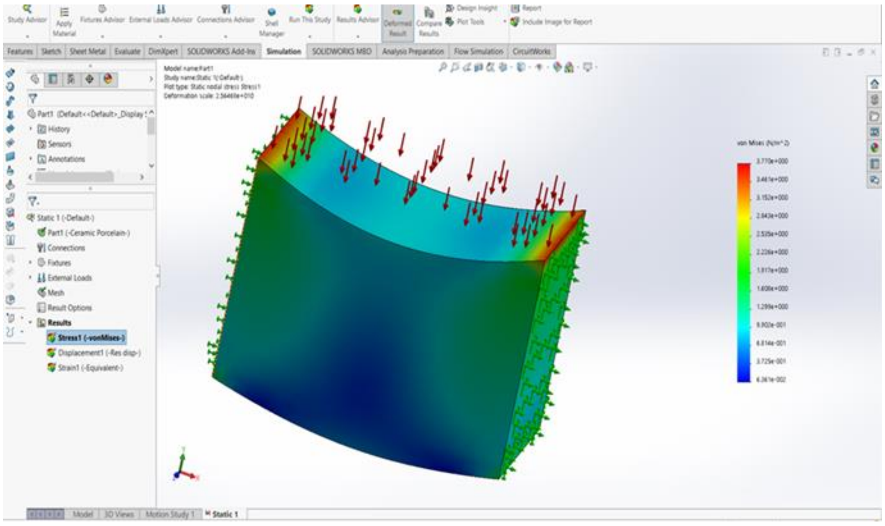

Fig. 4. *Simulating the compression forces on the walls of the tundish by applying the ABAQUS program*

The program also allows the creation of samples, on which the compression resistance is simulated.

The specimen is drawn in 3D, in the form of a cylinder with dimensions 150 mm X 375 mm with a fixed end, and the material used is concrete.

After applying pressure, from the upper part of the cylinder, a tension force is generated, which leads to the generation of cracks. Through this concrete compression test, we can find out the pressure value that the material at hand can withstand (Fig. 5).

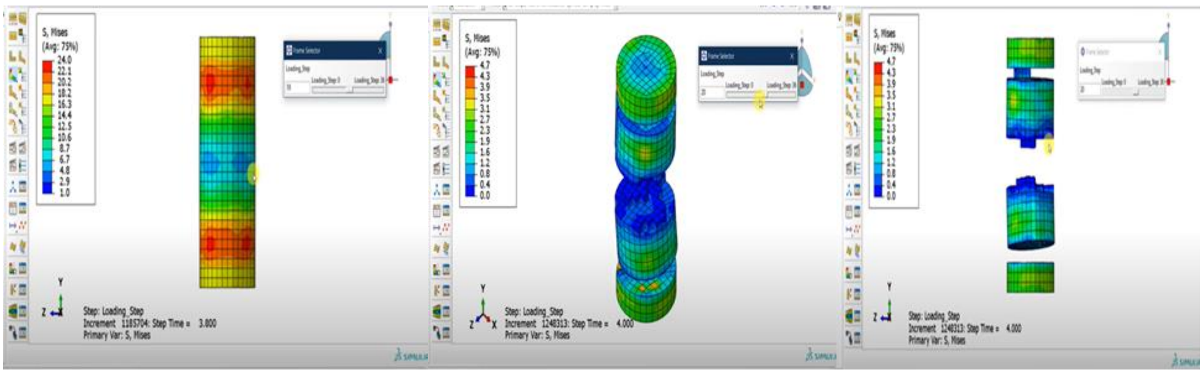

Fig. 5. *Sequences, of the application of the SolidWorks and ABAQUS programs, for determining the compressive strength of the refractory concrete, from the lining of the tundish*

The compression forces, which act on the walls of the tundish, developed by the liquid alloy, combined with the temperature differences, and with the friction, which occurs at the interface of the alloy with the shotcrete layer, represent an important factor that can influence the quality of the steel, through liner wear of the tundish.

4. Conclusions

The topological optimization of the tundish would represent a solution for increasing the quality of continuous cast steel.

The simulation of the movement of the liquid alloy in the tundish highlights the erosion of its refractory lining.

The RealFlow program is a tool for simulating fluids in a dynamic system, with the help of which you can observe the filling mode of the tundish, highlighting the first contact area of the jet with the tundish wall, and the "dead" areas, as well as the turbulences. These can appear during the flow and can have a negative impact on the quality of the steel in the tundish.

During the operation of changing the casting pots, inclusions are generated because there is a period of temperature fluctuation and of the equilibrium state, which can lead to the reoxidation of the melt, to reactions with the casting slag, and to the deposition of masonry particles to the casting pot.

References

[1]. McLean A., *The Turbulent Tundish-Contaminator or Refiner*, Proc. Steelmaking Conf., Iron and Steel Society, 71, p. 3-23, 1988.

[2]. Van der Stel J., *et al.*, *Tundish Metallurgy: A Solution or a Limitation to Clean Steel*, Development in Ladle Steelmaking and Continuous Casting, edited by G. D. Lawson (Montreal: The Canadian Institute of Mining and Metallurgy, p. 218-223, 1990.

[3]. Lowry M. L., Sahai Y., *Thermal Effects on the Flow of Liquid Steel in Continuous Casting Tundishes*, Iron and Steelmaker, 19:3, p. 81-88, J. Schade. Lecture Notes, ISS Short Course on Ladle and Tundish Metallurgy for Clean Steels, p, 314-321, Oct. 10, 1997.

[4]. Sahai Y., Chakraborty S., *Importance of Thermal Modeling in Continuous Casting Tundishes*, Proc. Process Technology Division Conf., 10, p. 161-176, 1992.

[5]. Graves A. M., *et al.*, *Design of Consumable Tundish Refractories for Production of UltraLow-Carbon Steel*, Proc. Steelmaking Conf., 75, p. 333-335, 1992.

[6]. Daussan A., Martin J., Roziere J., Steel Purity in Continuous Casting Tundishes, Proc. Steelmaking Conf., 78, p. 471-477, 1995.

[7]. Dorricott J. D., Heaslip L. J., Hoagland P. J., *Asymmetric Tundish Design and Flow Control Principles in Multistrand Billet and Bloom Casters*, Proc. Electric Furnace Conf., Iron and Steel Society, 48, p. 119-124, 1990.

[8]. Hiraki S., *et al.*, *Influence of Tundish Operations on the Quality of Hot Coils During HighSpeed Continuous Casting*, Iron & Steelmaker, 26:3, p. 47-52, 1999.

[9]. Suzuki I., *et al.*, *Development of Tundish Induction Heater for High Quality Continuously Cast Blooms*, Tundish Metallurgy, vol. 1, edited by A. McLean (Warrendale, Pa.: Iron and Steel Society), p. 201-207, 1990.

[10]. Melville S. D., Brinkmeyer L., *Evaluating Steelmaking and Casting Practices Which Affect Quality*, Proc. Steelmaking Conf., 78, p. 563-569, 1995.

[11]. McPherson N. A., McLean A., *Tundish to Mold Transfer Operations*, Continuous Casting, vol. 6 (Warrendale, Pa.: Iron and Steel Society), p. 11-15, 1992.

THE ANNALS OF "DUNAREA DE JOS" UNIVERSITY OF GALATI
FASCICLE IX. METALLURGY AND MATERIALS SCIENCE
Nº. 1 - 2023, ISSN 2668-4748; e-ISSN 2668-4756
Article DOI: https://doi.org/10.35219/mms.2023.1.04

CORROSION INHIBITION EFFICACY OF HYBRID ORGANIC EXTRACTS FROM *PROSOPISAFRICANA* AND *CITRULLUSLANATUS* ON MILD STEEL IN ACIDIC MEDIUM

Yusuf Lanre SHUAIB-BABATA[1*], Israel Victor AYINDE[1], Yusuf Olanrewaju BUSARI[1], Mubarak Oloduowo AMEEN[2], Raheem Abolore YAHYA[1], Ibrahim Owolabi AMBALI[1], Ishaaq Na'allah AREMU[1], Sikiru Ottan ABDULRAMAN[3], Kabiru Suleiman AJAO[1], Abdulateef Alabi GARUBA[4]

[1]Department of Materials & Metallurgical Engineering, University of Ilorin, Nigeria
[2]Department of Mechanical Engineering, University of Ilorin, Ilorin, Nigeria
[3]Department of Material Science and Engineering, Kwara State University Malete, Nigeria
[4]Department of Mechanical Engineering, Kwara State Polytechnic, Ilorin, Nigeria
e-mail: sylbabata@unilorin.edu.ng; sylbabata2@gmail.com

ABSTRACT

Each of Prosopis Africana pod extract (PAPE) and Citrulluslanatus (WMPE) performed quite well as green inhibitors in the electrochemical corrosion in acidic solution at ambient temperature in previous research. However, the hybridization of these compounds was varied with the concentration ratio in this study to optimize the efficiency of the green inhibitor in a hydrochloric acid medium using mild steel. The extraction process of the inhibitor samples was carried out with the Soxhlet apparatus using n-hexane as the solvent. Furthermore, the potential inhibition efficiency was monitored using various corrosion measurement techniques at room temperature. The inhibitive response of the extracts could be attributed to the adsorption of the extracts' components on mild steel surface by physisorption mechanism according to the Langmuir adsorption isotherm model. The results revealed that inhibition efficiency (IE%) depends on the concentration of the extracts. The peak IE% values were obtained with a hybrid ratio of 3:1 (PAPE: WMPE) for gravimetric technique. The Tafel polarization and gasometrical measurement technique is 96.7%, 98.5% and 83.1% respectively at the concentration of 1.0 g/L, which are above the peak IE% for PAPE (93.7%, 80.96% and 77.8%) and WMPE (92.7%, 80.5% and 75.6%).

KEYWORDS: hybrid, green inhibitor, prosopis africana, citrulluslanatus, inhibition efficiency

1. Introduction

The major degradation mechanism of mild steel in environmental operations is corrosion. Steel corrosion has been the subject of several studies due to its low-cost, wide range of mechanical properties, and industrial applications especially in steel structures. The consequences of this electrochemical reaction affect the safe reliability and effective operation of metal components or equipment and are frequently more severe than the mere loss of a quantity of metal [1]. Organic inhibitors have effectively isolated the metal from corrosion agents [2] since the inorganic compounds endanger the ecosystem [3-5]. One of the challenges of selecting the type of inhibitor has been to develop a scalable particular with approach to identify sustainable bio-material that portends excellent inhibition. Therefore, the inhibitor composition determined the efficiency which includes the size of the molecule, the amount and node of adsorption molecule, the charge density, metallic complexes formation, and the inhibitor's intended area of the metal surface; notwithstanding, characteristics of the environment and the nature of electrochemical potential at the interface [6, 7].

THE ANNALS OF "DUNAREA DE JOS" UNIVERSITY OF GALATI
FASCICLE IX. METALLURGY AND MATERIALS SCIENCE
N°. 1 - 2023, ISSN 2668-4748; e-ISSN 2668-4756
Article DOI: https://doi.org/10.35219/mms.2023.1.04

Based on the hazardous effect of most synthetic corrosion inhibitors, a lot of scientists have considered research on the use of natural biodegradable materials and some agricultural products and wastes can be used as corrosion retardation since they are economical, easily accessible, and renewable sources of materials, as well as being environmentally safe and ecologically tolerable [8-11]. The corrosion inhibitive capacities of Prosopis Africana and watermelon peel in 1 M Hydrochloric (HCl) acid medium for low carbon steel grades have been reported separately. This is monitored with gravimetric and Tafel polarization method in PAPE, analysing the corrosion inhibition and protection of zinc in natural seawater by watermelon peel respectively [2, 12-16]. There are just a few accounts in the specialised literature on using Prosopis Africana and watermelon components for corrosion inhibition. The existing research on plant extracts as corrosion inhibitors mainly focuses on specific plant components such as leaves, stems, bark, roots, and fruits. However, hybridizing research on extracts from diverse components of a certain plant for corrosion inhibition is limited. In furtherance to the studies on the development of green corrosion inhibitors, this study investigates the inhibiting effect of hybridizing Prosopis Africana pod and watermelon peel extract in different ratios on the corrosion of mild steel in 1M HCl solution using gravimetric analysis, gasometric analysis, and Tafel polarization methods.

2. Experiments

2.1. Preparation of inhibitor extracts

The Prosopis Africana pod and the watermelon peels were air dried and ground into a fine powder. The extractions of the samples were carried out in the Department of Chemistry, University of Ilorin, Ilorin, Nigeria. The samples were extracted on a Soxhlet apparatus with n-hexane as the solvent. The extracts were utilized to make stock solutions, which were then used to evaluate the corrosion inhibition properties independently and in combination. Samples of each stage in preparing the inhibitor extract are presented in Figure 1.

2.2. Materials Preparation

Mild steel sourced in the local market with elemental composition analysed at Midwal Engineering Service Limited in Lagos, Nigeria using Spectromaxx LMF06 Spectrometer. The 2.5 x 2.0 x 0.1 cm, coupons for the gravimetric test were prepared using ASTM G1-03 [17] and G4 standards [18] then polished, degreased in ethanol, dried in acetone, and then stored in a desiccator. For the corrosion study, an acidic solution was prepared by dilution of HCl (sp.gr.1.18) with distilled water.

Fig. 1. *The process of extraction of* Prosopis Africana *pod and watermelon peel*

2.3. Weight Loss Measurement/ Gravimetric Technique

The simplest technique of corrosion rate and inhibition efficiency is to use weight loss measurement. The test specimens were pre-weighed and totally immersed in 200 mL solutions of various concentrations prepared in 1.0 M HCl solution at (38 °C), with and without various proportions of Prosopis Africana pod extract and watermelon peel extract with the ratios: 2:1, 1:2, 3:1 and 1:3, sealed from the atmosphere using ASTM NACE/ASTM G31-12a guidelines [19]. The test specimens were exposed to the medium between 24 and 2,160 hours in accordance with guidelines in the ASTM G1 standard [17]. The experiment setup is shown in Figure 2. The specimens were removed after 24 hours, washed in distilled water, rinsed in ethanol and acetone, dried, and reweighted using an electronic weighing balance (HX 302 with 0.01 g accuracy). The process was repeated for other periods of exposure in the medium until 2,160 hours of observations. The corrosion rate was determined using Equation (1),

$$Corrosionrate(mpy) = \frac{kW}{ATD} \quad (1)$$

where W is the weight loss (g), A is the total area of metal specimen in cm^2, k = 3.45 x 10^6 mils per year (mpy), D is the density of steel (g/cm^3) and T is the immersion time (hours).

The calculated corrosion rate inhibition efficiency (I.E.%) was obtained by using the relationship in Equation (2),

$$I.E(\%) = \frac{CR_{Blank} - CR_{Inh}}{CR_{Blank}} \times 100 \quad (2)$$

where CR_{Blank} and CR_{Inh} is the corrosion rate of the mild steel specimens in the absence and presence of inhibitor respectively. The experimental setup and some specimens after the corrosion tests are shown in Figure 2.


(a)

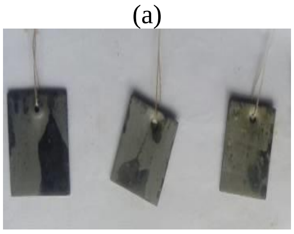
(b)

Fig. 2. *(a) Weight loss set-up and (b) cleansed specimen after corrosion test*

2.4. Hydrogen evolution (Gasometric) measurement

The volume of evolved hydrogen gas from corroded mild steel was measured using the hydrogen evolution measurement setup. A 200 mL of prepared environment (1 M HCl) was put into two-necked conical flasks and the burette beginning volume was set to 50 mL. To prevent gases from escaping, the test specimen from the desiccator was put into the HCl solution and tightly closed. The volume of hydrogen bubbles formed, as a result of the reaction between metal and acidic environment, which increased over 300 minutes. During the reaction, the volume was measured at 10-minute intervals and recorded with the downward displacement of water in the burette. This procedure was carried out for other prepared inhibition test solutions of different concentrations of the hybrid *Prosopis Africana* pod extract (PAPE) and watermelon peel extract (WMPE). The inhibition efficiency (I.E%) from the hydrogen evolution measurement was determined using Equation (3).

$$I.E\% = 1 - \frac{CR_{Inh}}{CR_{abs}} \times 100\% \qquad (3)$$

2.5. **Tafel** *polarization technique*

Tafel polarization experiments were carried out at room temperature utilizing a three-electrode cell configuration. Using a guillotine machine, mild steel of 1.0 cm^2 was employed as the working electrode, and a platinum electrode was used as an auxiliary electrode dimension. Using aluminium foil to hold it together, a flexible cable was linked to the specimen and placed on a cup mold. In another cup mold, a hardener was applied to a polyester resin and carefully combined. An accelerator was added to the mixture and the two were mixed together to form a solution. The prepared solution was then poured in the mold where the specimens were placed, and left for a period between 15 to 20 minutes to solidify. After solidification, they were removed from the mold. Before being exposed to the atmosphere, the coupon was further polished with several grades of emery sheets to achieve a gleaming reflective surface (like a mirror). The preparation of the specimen samples for the *Tafel* polarization procedures is shown in Figure 3.


(a)


(b)

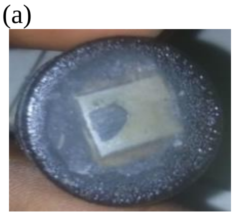
(c)

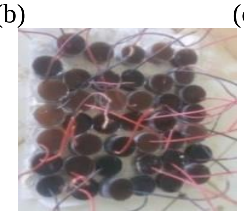
(d)

Fig. 3. *(a) Electrochemical measurement analysis setup (b) Connection of electrodes inside the medium (c) Mounted* Tafel *sample before polishing (d)* Tafel *samples ready for test*

3. Results and discussion

3.1. Elemental Composition Analysis

Elemental composition analysis of the steel sample results in weight percentage is presented in Table 1. By the American Iron and Steel Institute (AISI) classification of steel, the steel sample used in this study containing 0.0112% carbon falls within the class of low-carbon steel. Low-carbon steel is associated with very low carbon content, less than

THE ANNALS OF "DUNAREA DE JOS" UNIVERSITY OF GALATI
FASCICLE IX. METALLURGY AND MATERIALS SCIENCE
Nº. 1 - 2023, ISSN 2668-4748; e-ISSN 2668-4756
Article DOI: https://doi.org/10.35219/mms.2023.1.04

0.10% C [20-23]. Low-carbon steels with a carbon content less than 0.30% are called mild steels [24]. Low-carbon/mild steel contains carbon within the range of 0.05 and 0.25% [25].

Table 1. *Elemental composition of mild steel sample*

Fe	99.700%	**C**	0.0612%	**Mn**	0.1020%
P	0.0222%,	**Si**	0.0052%	**Cr**	0.0342%
Al	0.0134%	**Ni**	0.0015%	**Sn**	0.0053%
Co	0.0159%	**Ti**	0.0002%	**S**	0.0389%

3.2. Phytochemical Analysis

The results of the phytochemical screening of the *Prosopis Africana* pod and watermelon peel extracts are shown in Tables 2 and 3.

Table 2. *Phytochemical analysis result of* Prosopis Africana *pod*

Saponin	108.70	**Alkaloids**	101.60
Tannin	83.80	**Phenol**	9.90
Steroids	7.80	**Flavonoid**	2.10
Cardiac cilycosides		1.06	

Table 3. *Phytochemical analysis result of watermelon peel*

Citrulline	+	**Alkaloid**	+
Flavonoids	+	**Terpenoids**	+
Tannin	-	**Polyphenol**	+
Saponin	+		

It can be deduced from the results in Table 2 that Saponin, Alkaloids, and Tannin are the most abundant constituent in *Prosopis Africana* and are the most powerful components in the pod for inhibiting corrosion, which is in line with the findings in previous studies [2, 13, 26, 27]. For the watermelon peel, out of the constituent tested for, only tannin was found negative while other constituents (citrulline, flavonoids, tannin, saponin, alkaloid, terpenoids, and polyphenol) were present and served as the corrosion inhibiting agents of the extract on mild steel.

3.3. Gravimetric Technique (Weight loss)

The results of corrosion rate values are plotted against the exposure time for the hybrid concentration of inhibitors in different ratios of PAPE and WMPE (100%, 3:1, 1:3, 2:1, and 1:2 in Figures 5-10). The specimens during the electrochemical tests performed using acidic media are observed without corrosion inhibitor (0.0 g/L) corroded at a higher rate if this behaviour is compared against the specimens. Furthermore, as the concentration of the extract increases, the corrosion rate of the test specimen decreases significantly. The reduction in corrosion rate could be ascribed to the phytochemicals adhering to the metal's surface, forming a barrier to the metal's disintegration in the corrosive medium [26].

At 100% PAPE green inhibitor in Figure 5, after 2160 hours, 1.0 g/L recorded 130.05 mpy. Also in Figure 6, similar trends but slightly lower values were observed for 100% of WMPE. Figure 7, PAPE: WMPE ratio 3:1 result shows a drastic decrease in corrosion rate with time exposure up to 2160 hours. However, the 1:3 concentration ratio of PAPE:WMPE in Figure 8 recorded an increase corrosion rate along the exposure time. This shows that the corrosion rate is highly dependent on the concentration of the inhibitor.

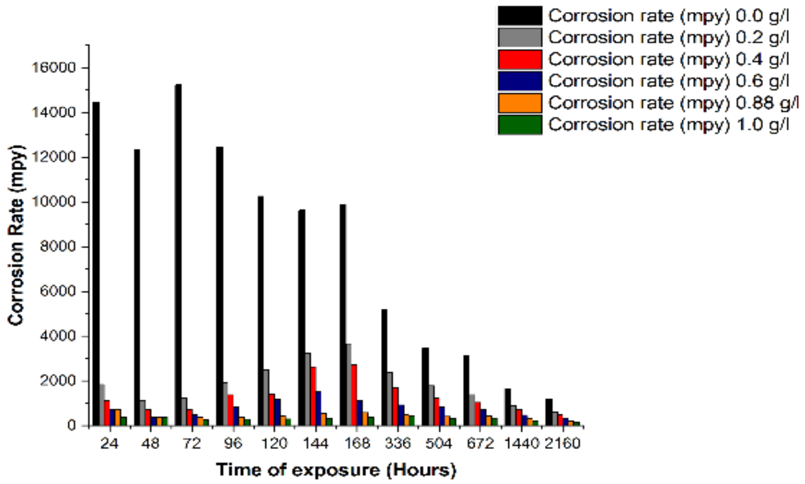

Fig. 4. *Corrosion rate (mpy) for 100% PAPE concentration ratio*

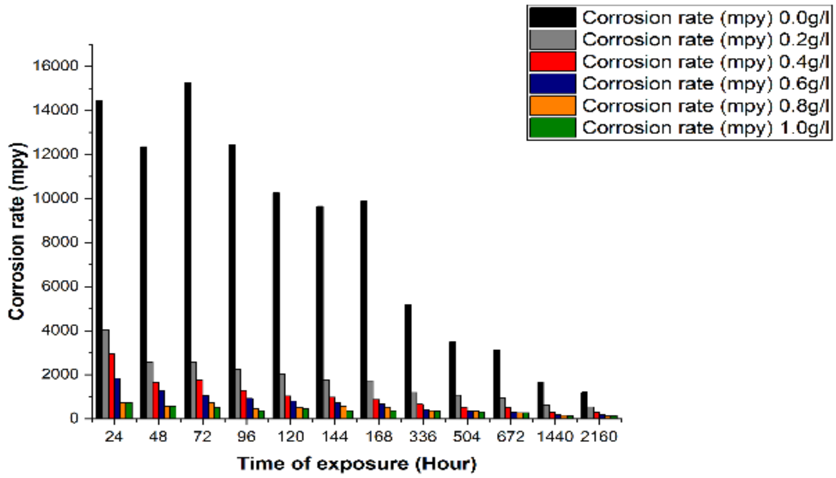

Fig. 5. *Corrosion rate (mpy) for the 100% WMPE concentration ratio*

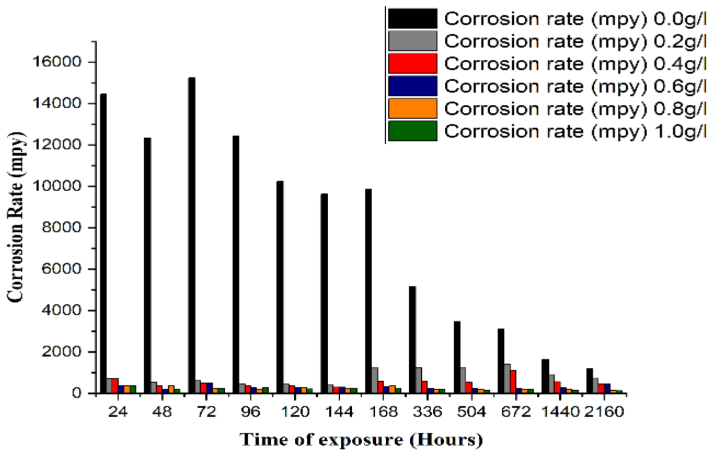

Fig. 6. *Corrosion rate (mpy) for the 3:1 concentration ratio of PAPE:WMPE*

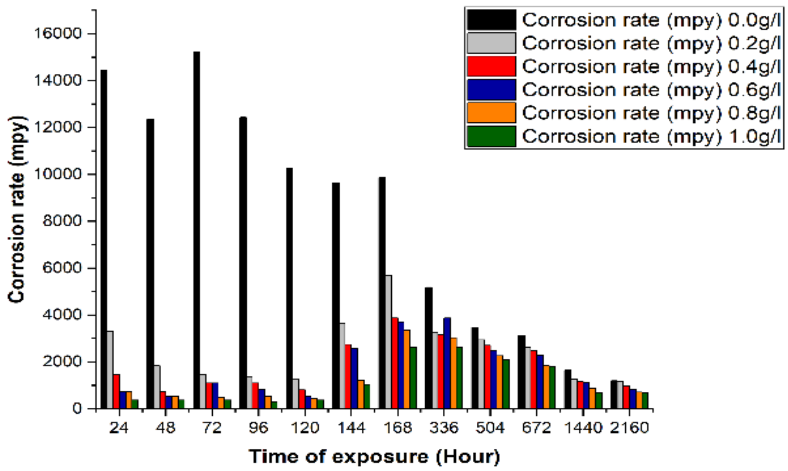

Fig. 7. *Corrosion rate (mpy) for the 1:3 concentration ratio of PAPE:WMPE*

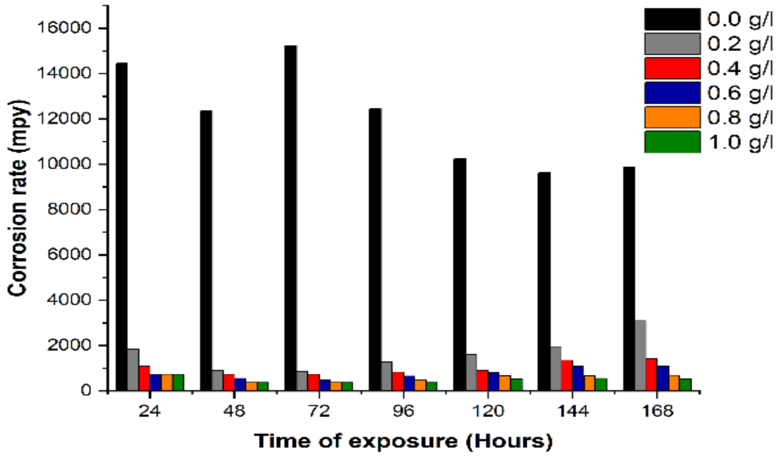

Fig. 8. *Corrosion rate (mpy) for the 2:1 concentration ratio of PAPE:WMPE*

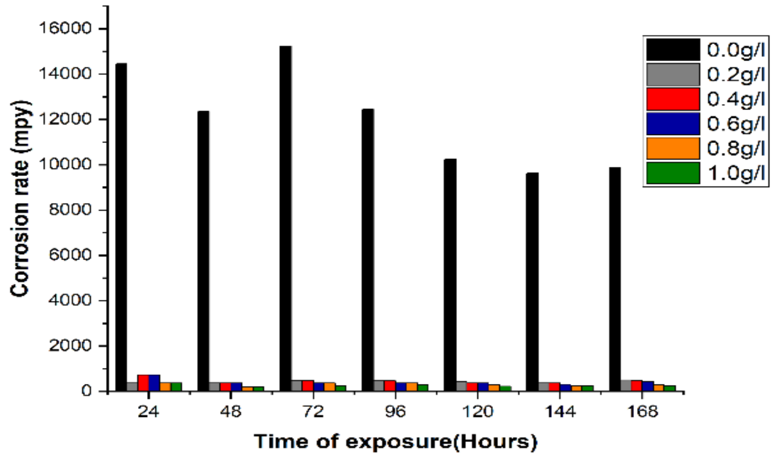

Fig. 9. *Corrosion rate (mpy) for the 1:2 concentration ratio of PAPE:WMPE*

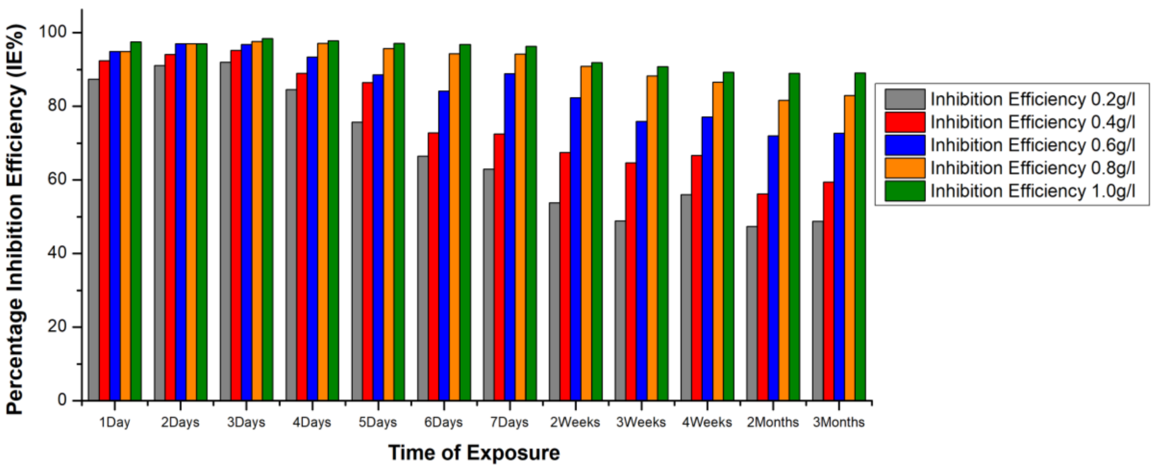

Fig. 10. *Percentage Inhibition Efficiency for the 100% PAPE concentration ratio*

THE ANNALS OF "DUNAREA DE JOS" UNIVERSITY OF GALATI
FASCICLE IX. METALLURGY AND MATERIALS SCIENCE
N°. 1 - 2023, ISSN 2668-4748; e-ISSN 2668-4756
Article DOI: https://doi.org/10.35219/mms.2023.1.04

The trends of inhibitory efficiency (IE%) for hybrid concentrations of PAPE and WMPE are illustrated in Figures 11-16. This was used to examine the extracts' potential for inhibitive behavior. It is shown that increasing the inhibitor concentration increases inhibition efficiency. However, this was not consistent with the period of exposure. The efficiency is attributed to the development of a protective coating due to the change of the metal/solution interface from an active to a passive dissolution state [26].

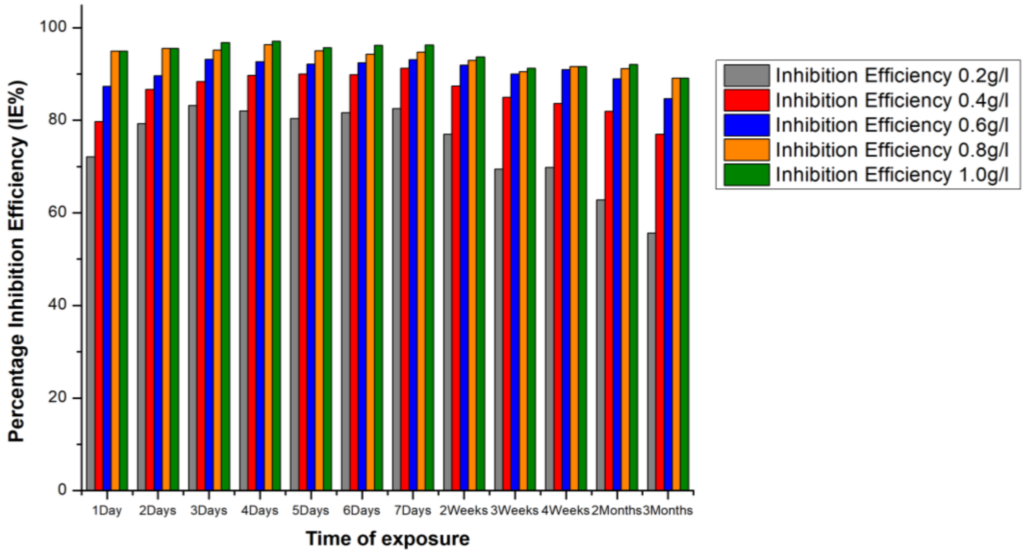

Fig. 11. *Percentage Inhibition Efficiency for the 100% WMPE concentration ratio*

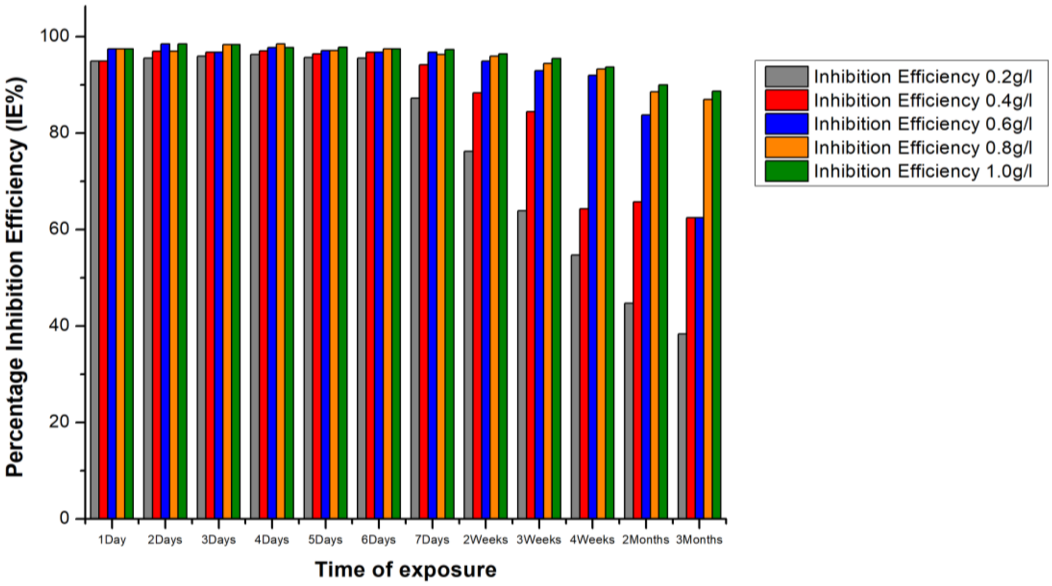

Fig. 12. *Percentage Inhibition Efficiency for the 3:1 concentration ratio of PAPE:WMPE*

THE ANNALS OF "DUNAREA DE JOS" UNIVERSITY OF GALATI
FASCICLE IX. METALLURGY AND MATERIALS SCIENCE
N°. 1 - 2023, ISSN 2668-4748; e-ISSN 2668-4756
Article DOI: https://doi.org/10.35219/mms.2023.1.04

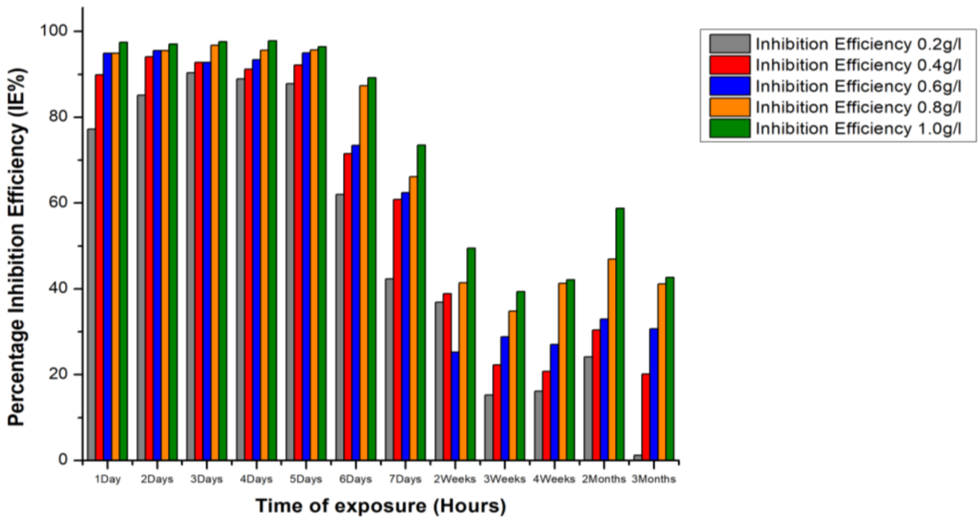

Fig. 13. *Percentage Inhibition Efficiency for the 1:3 concentration ratio of PAPE:WMPE*

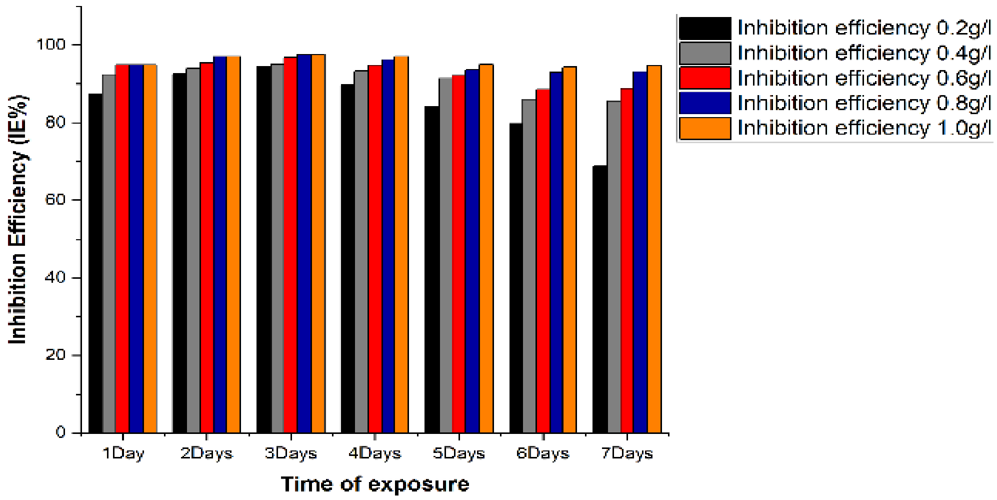

Fig. 14. *Percentage Inhibition Efficiency for the 2:1 concentration ratio of PAPE:WMPE*

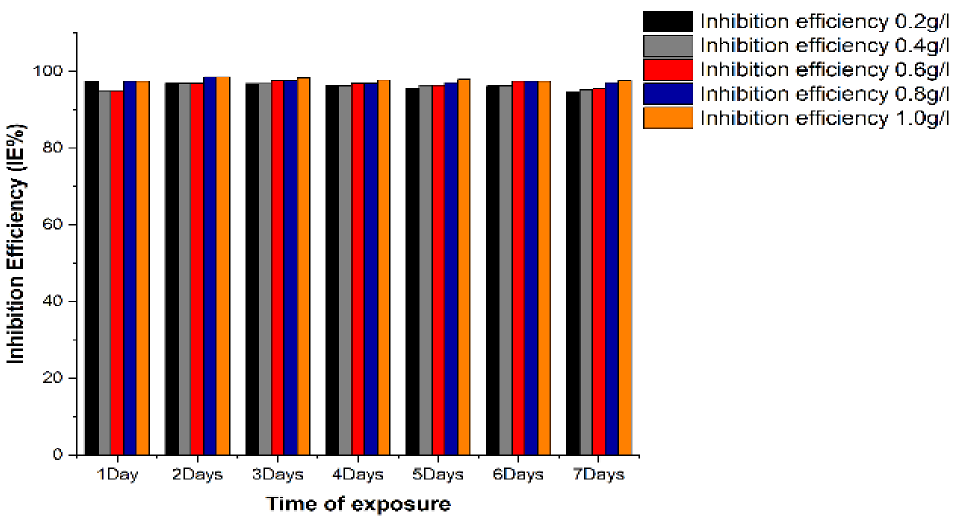

Fig. 15. *Percentage Inhibition Efficiency for the 1:2 concentration ratio of PAPE:WMPE*

Nº. 1 - 2023, ISSN 2668-4748; e-ISSN 2668-4756
Article DOI: https://doi.org/10.35219/mms.2023.1.04

Through the gravimetric measurement technique, the peak inhibition efficiency value of 96.7% was obtained at the concentration of 1.0 g/L with 3:1 PAPE:WAPE, which is above the inhibition value obtained with PAPE (93.7%) and WMPE (92.7%).

3.3. Hydrogen evolution measurement

The volume of hydrogen gas evolved in the presence and absence of different concentrations of the hybrid extracts that are presented in Figures 16-20. The results showed that the volume of evolved hydrogen gas increases with time but decreases with an increase in the concentration of the extracts. For example, after 300 minutes of observation, the highest and lowest reading for evolved hydrogen was recorded for PAPE, WMPE, 3:1 of PAPE: WMPE and 1:3 of PAPE:WMPE in 0.0 g/L (27.00 for all considerations) and 1.0 g/L (5.20, 7.10, 4.10 and 4.90 respectively). The result affirms the view of Odusote *et al.* [26] that the evolution rate of gas decreases as the concentration increases. This may be a result of the formation of a passive layer on the surface of the metal in the extract inhibitor.

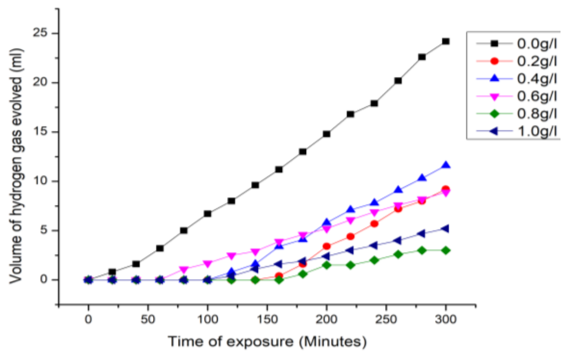

Fig. 16. *Rate of evolution of hydrogen gas in 1 M HCl at different concentrations of the 100% PAPE*

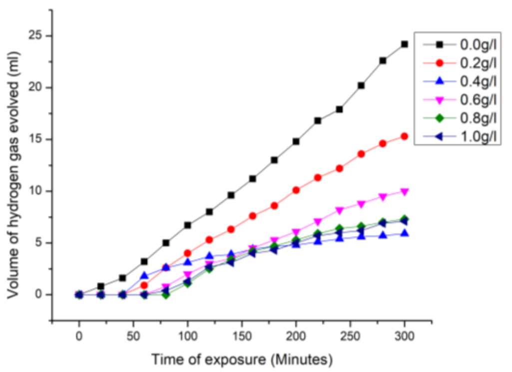

Fig. 17. *Rate of evolution of hydrogen gas in 1 M HCl at different concentrations of the 100% WMPE*

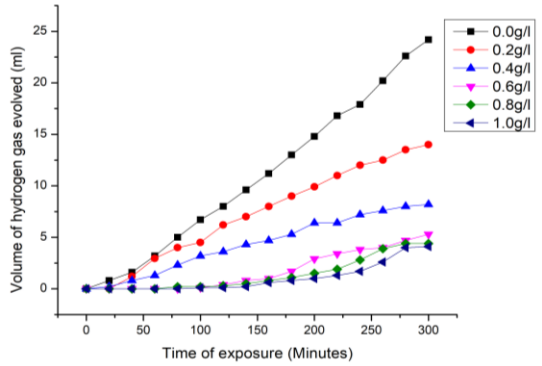

Fig. 18. *Rate of evolution of hydrogen gas in 1 M HCl at different concentrations of the 3:1 hybrid extract*

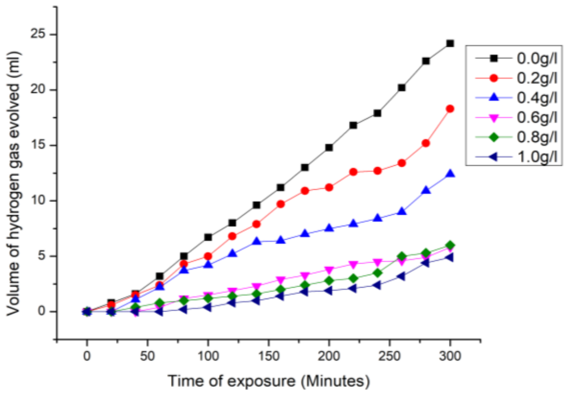

Fig. 19. *Rate of evolution of hydrogen gas in 1 M HCl at different concentrations of the 1:3 hybrid extract*

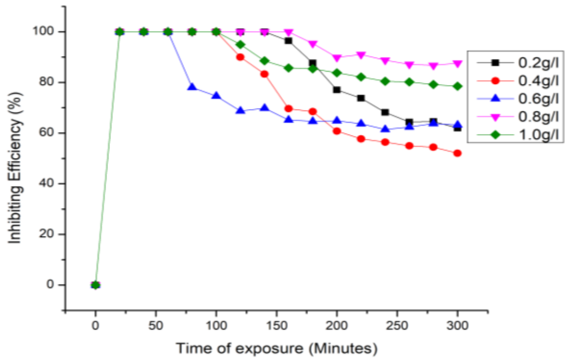

Fig. 20. *Variation of inhibition efficiency with time of exposure at different concentrations of 100% PAPE*

THE ANNALS OF “DUNAREA DE JOS” UNIVERSITY OF GALATI
FASCICLE IX. METALLURGY AND MATERIALS SCIENCE
Nº. 1 - 2023, ISSN 2668-4748; e-ISSN 2668-4756
Article DOI: https://doi.org/10.35219/mms.2023.1.04

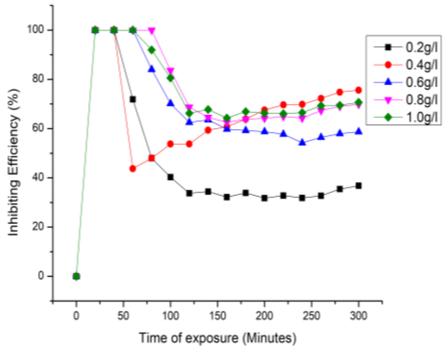

Fig. 21. *Variation of inhibition efficiency with time of exposure at different concentrations of 100% WMPE*

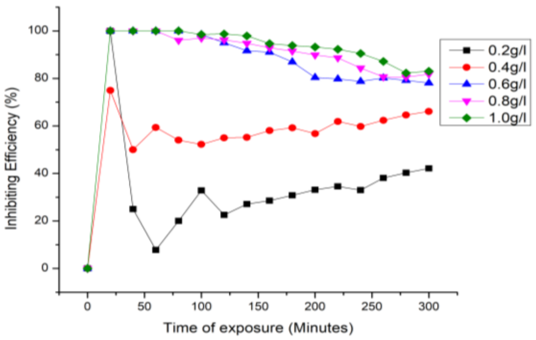

Fig. 22. *Variation of inhibition efficiency with time of exposure at different concentrations of 3:1 Hybrid*

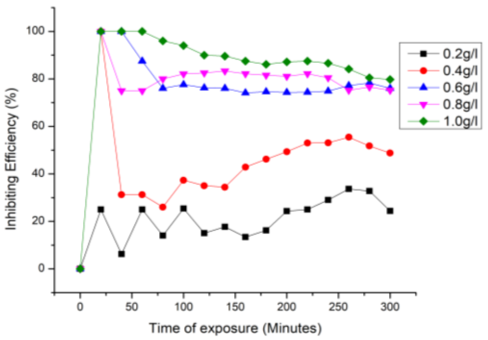

Fig. 23. *Variation of inhibition efficiency with time of exposure at different concentrations of 1:3 Hybrid*

Figures 21-24 show the results obtained by the variation of percentage inhibition efficiency with the time of exposure. The results show that when the concentration of the inhibitors’ extracts increases, the inhibition efficiency increases. The extracts' physiochemical components may be responsible for corrosion inhibition. At 1.0 g/L, the maximum inhibitory efficiency (83.1%) was recorded.

3.4. Tafel *polarization*

Figures 24-27 show the curves derived from the *Tafel* polarization measurements of mild steel dissolution in 1 M of HCl in the absence and presence of various amounts of hybrid inhibitors. In the presence of PAPE, WMPE, and hybrid inhibitors, both anodic and cathodic current densities were reduced, indicating a mixed-type inhibitor activity [2, 15]. As the concentration of the extracts increases, the Icorr values are reduced. It can be seen that as the extract concentration rises, the inhibition efficiency rises as well. The influence of the extract on both anodic and cathodic reactions is seen in this result. The highest inhibition efficiency was obtained at 1.0 g/L of the hybrid inhibitors of the ratio of PAPE to WMPE in ratios of 3:1, 1:3, 2:1, and 1:2 which give the result of 98.52%, 80.95%, 82.35% and 97.41% respectively. This implies that the most appropriate ratio in the formulation of an effective hybrid organic inhibitor comprising of PAPE and WMPE was achieved at the ratio 3:1 PAPE:WMPE.

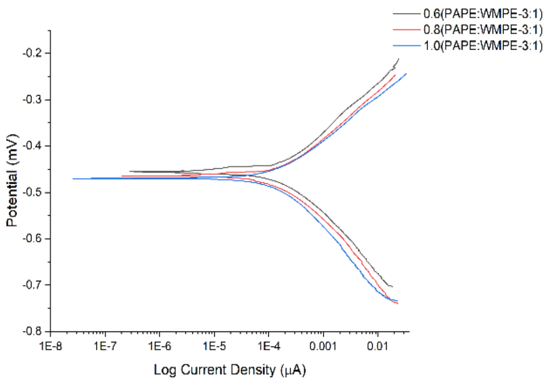

Fig. 24. *Tafel Polarization curves of mild steel in 1 M HCl with and without both PAPE and WMPE Inhibitor in ratio of 3:1*

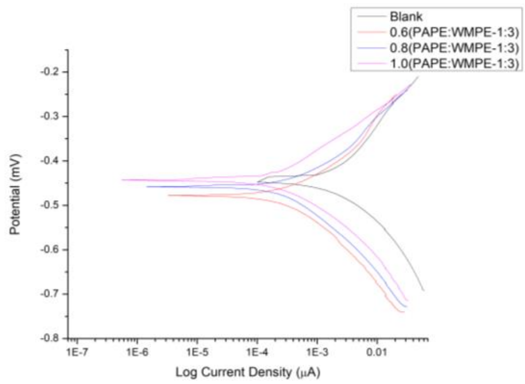

Fig. 25. *Tafel Polarization curves of mild steel in 1 M HCl with and without both PAPE and WMPE Inhibitor in ratio of 1:3*

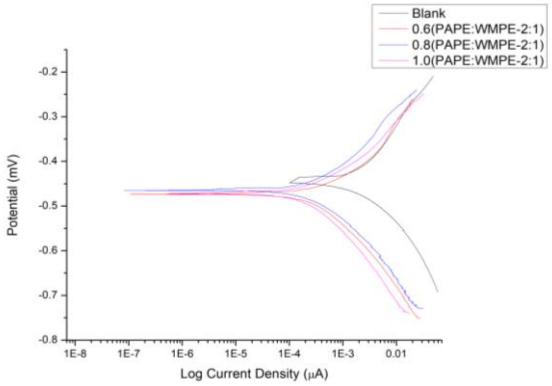

Fig. 26. *Tafel Polarization curves of mild steel in 1 M HCl with and without both PAPE and WMPE Inhibitor in ratio of 2:1*

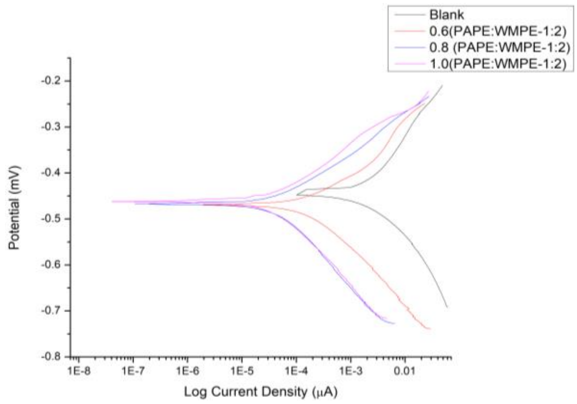

Fig. 27. *Tafel Polarization curves of mild steel in 1 M HCl with and without both PAPE and WMPE Inhibitor in ratio of 1:2*

From Figures 24-28 showing the results of PAPE and WMPE *Tafel* polarization, it is observed that the corrosion potentials (Ecorr) for the mild steel in the presence of PAPE all shifted toward the negative potentials. As the concentration of the extracts increases, the corrosion current density (Icorr) values decreased. However, the inhibition efficiency value computed from the corrosion current density in the absence (Icorro) and presence (Icorr) of the inhibitor increased. The highest inhibition efficiency of 98.52 % was obtained at 1.0 g/L concentration. The shift in the *Tafel* slopes of both the cathodic reaction (βc) and anodic reaction (βa) as shown in Figures 24-28 in the presence and absence of the extract suggests that the inhibitor affects both the cathodic and anodic reactions. This also implies that the hybrid extract is a mixed inhibitor. Some of the components included in the examined extracts may be protonated in the HCl solution, and these protonated species may adsorb directly on the mild steel surface's cathodic sites. According to Odusote *et al.* (2016), the inhibitory mechanism was activated by simply blocking the available cathodic and anodic sites on the metal surface.

4. Conclusions

The following conclusions were drawn from the investigation into the inhibition of mild steel corrosion in hydrochloric acid solution by hybridizing Prosopis Africana pod and watermelon peel extract using weight loss measurement, hydrogen evolution measurement, and *Tafel* polarization techniques:

i. The corrosion rate of the mild steel in the HCl solution was found to decrease with an increase in the concentration of the entire ratio considered.
ii. The inhibiting efficiency of the entire ratio considered is dependent on the concentration of the extract and it increased with the increase of concentration of the extract in the acidic medium irrespective of the corrosion measurement technique used.
iii. All ratio hybrid inhibitor extracts could serve as an effective inhibitor of corrosion of mild steel in hydrochloric acid solution. Meanwhile, the hybrid of the two green inhibitors of a ratio of 3:1 PAPE: WMPE displayed the best IE% (98.52%), followed by a hybrid ratio 1:3 with IE% of 97.79%, at a 1.0 g/L concentration after exposure in the 1M HCl medium for mild steel.
iv. The *Tafel* polarization technique results showed that extracts of each ratio hybrid inhibitor products acted as mixed-typed inhibitors via simple adsorption of the phytochemicals present in the extract on the mild steel surface in HCl solution, thereby influencing both cathodic and anodic mild steel dissolution reactions as revealed by the *Tafel* polarization measurements.

Acknowledgments

The authors express their profound gratitude and appreciation to the management of Midwal Engineering Limited, Lekki, Lagos State, Nigeria for their support by allowing us to use their laboratory facilities for some of the tests carried out in this study.

References

[1]. Bradford S. A., Bringas J. E., *Corrosion control*, col. 115, Springer, 1993.
[2]. Odewunmi N., Umoren S., Gasem Z., *Watermelon waste products as green corrosion inhibitors for mild steel in HCl solution*, Journal of Environmental Chemical Engineering, 3(1), p. 286-296, 2015.

[3]. Thangamalathi S., Anuradha V., *Role of inorganic pollutants in freshwater ecosystem - A review*, International Journal of Advanced Research in Biological Sciences, 5(11), p. 39-49, 2018.

[4]. Anne Th. S., Jes J. R., Sebastian H., Walter T., Poul L. B., Ursula S. M., *Linking ecological health to co-occurring organic and inorganic chemical stressors in a groundwater-fed stream system*, Science of the Total Environment, 642, p. 1153-1162, 2018.

[5]. Howe P. D., Malcolm H. M., Dobson S., *Manganese and its compounds: environmental aspects*, The Centre for Ecology & Hydrology, Monks Wood, United Kingdom; United Nations Environment Programme; International Labour Organization, and the World Health Organization, Geneva.

[6]. Okafor P. C., Liu C. B., Liu X, Zheng Y. G., *Inhibition of CO_2 corrosion of N80 carbon steel by carboxylic quaternary imidazoline and halide ions additives*, Journal of Applied Electrochemistry, 39, p. 2535-43, 2009. https://doi.org/10.1007/s10800-009-9948-5.

[7]. Kadhim A, Betti N, Gaaz T., *A mini review on corrosion, inhibitors and mechanism types of mild steel inhibition in an acidic environment*, International Journal of Corrosion and Scale Inhibition, 10, p. 861-84, 2021, https://doi.org/10.17675/2305-6894-2021-10-3-2.

[8]. Singh A., Singh V., Quraishi, M., *Effect of fruit extracts of some environmentally benign green corrosion inhibitors on corrosion of mild steel in hydrochloric acid solution*, Journal of Materials and Environmental Science, 1(3), p. 162-174, 2010.

[9]. Abeng F. E., Ekpe U. J., IkeubaA. I., UgiB. U., Nna P. J., *Inhibitive action of alkaloids and non alkaloid fractions of the ethanolicextracts of phyllanthusamarus on the corrosion of mild steel in HCl solution*, Global Journal of Pure and Applied Sciences 19, p. 107-117, 2013.

[10]. Singh A., Quraishi M. A., *The extract of Jamun (Syzygium cumini) seed as green corrosion inhibitor for acid media*, Research on Chemical Intermediates 41, p. 2901–14, https://doi.org/10.1007/s11164-013-1398-3, 2013.

[11]. Al-Amiery A. A., Kassim F. A. B., Kadhum A. A. H., Mohamad, A. B., *Synthesis and characterization of a novel eco-friendly corrosion inhibition for mild steel in 1 M hydrochloric acid*, Scientific reports, 6, p. 19890, 2016.

[12]. Petchiammal A., Rani P., Selvaraj S., Kalirajan K., *Corrosion protection of zinc in natural seawater using Citrullus vulgaris peel as an inhibitor*, Res. J. Chem. Sci., 2231, 606X, 2012.

[13]. Shuaib–Babata Y. L., Ibrahim H. K., Ambali I. O., Yahya R. A., Ajao K. S., Aremu N. I., Pelumi A. A., *Inhibitive potential of prosopis Africana on corrosion of low carbon steel in 1 M hydrochloric acid medium*, International Journal of Engineering Materials and Manufacture, 4(2), p. 66-76, DOI:10.26776/ijemm.04.02.2019.04, 2019.

[14]. Shuaib-Babata Y. L., Ibrahim H. K., Busari Y. O., Mahamood R. M., Abdulraman S. O., Ambali I. O., Abdulqadir B. L., Aremu I. N., Ajao K. S., Ejiko S. O., *Modelling of corrosion inhibition of cucumber plant extracts on AISI 1007 steel in sea water*, The Annals of "Dunarea De Jos" University of Galati, Fascicle IX. Metallurgy and Materials Science, 45 (1), p. 15-21, 2022.

[15]. Shuaib-Babata Y. L., Ayinde I. V., Ameen M. O., Busari Y. O., Ambali I. O., Abdulraman S. O., Ajao K, S., *Performance and corrosion inhibitive mechanism of Prosopis Africana pod extracts on mild steel in acidic medium*, Uniport Journal of Engineering and Scientific Research (UJESR), 6 (2), p. 34-43, 2022.

[16]. Al-Senani G. M., *Corrosion inhibition of carbon steel in acidic chloride medium by cucumissativus (cucumber) peel extract*, International Journal of Electrochemical Science 11, p. 291-302, 2016.

[18]. ***, ASTM G4 - 95, *Standard guide for conducting corrosion coupon test in field application*, p. 44-53, United States: ASTM International, 100 Barr Harbor Drive, West Conshohocken, PA 19428-2959, 1995.

[19]. ***, ASTM G1 - 03, *Standard practice for preparing, cleaning, and evaluation corrosion test specimens*, p. 14-21, United States: ASTM International, 100 Barr Harbor Drive, West Conshohocken, PA 19428-2959, 2003.

[20]. ***, NACE/ ASTM G31- 12a, *Standard guide for laboratory immersion corrosion testing of metals*, United States: ASTM International, 100 Barr Harbor Drive, West Conshohocken, PA 19428-2959, 2012.

[20]. Bruce R. S., *Introduction to the selection of carbon and low-alloy steels, In Welding, brazing, and soldering* (David L. O., Thomas A. S., Stephen L., Glen R. E. Eds), vol. 6, ASM International, DOI: https://doi.org/10.31399/asm.hb.v06.a0001404, 1993.

[21]. Michael E. M., David E. L., *Phase diagram and physical properties of low-C Steels, in physical metallurgy (Fifth edition)*, Elsievier, United States of America, 2014.

[22]. Jon L. D., *Classification of carbon and low-alloy steels, in practical heat treating: basic principles*, ASM International, ASM Technical Books DOI: https://doi.org/10.31399/asm.tb.phtbp.t59310095, 2020.

[23]. ***, Total Materia, *Classification of carbon and low-alloy steels*, Retrieved from https://www.totalmateria.com/page.aspx?ID=CheckArticle&site=kts&NM=62, Accessed on January 21, 2023.

[24]. Bob C., *Carbon metal content, Classification of Steel and Alloy Steels*, Retrieved from https://www.thefabricator.com/thewelder/article/metalsmaterials/carbon-metal-content-classification-of-steel-and-alloy-steels, Accessed on January 21, 2023.

[25]. Leeco Steel, *The Different Categories of Carbon Steel Plate: What is Carbon Steel?*, Retrieved from https://www.leecosteel.com/news/post/carbon-steel-categories/, Accessed on January 21, 2023.

[26]. Odusote J. K., Owalude D., Olusegun S., Yahya, R., *Inhibition efficiency of moringa oleifera leaf extract on the corrosion of reinforced steel bar in HCl solution*, The West Indian J. Eng, 38(2), p. 64-70, 2016.

[27]. Shuaib-Babata Y. L., Busari Y. O., Yahya R. A., Abdul J. M., *Corrosion inhibition of AISI 1007 steel in hydrochloric acid using cucumissativus (cucumber) extracts as green inhibitor*, ACTA Technica Corviniensis – Bulletin of Engineering, XI(4), p. 153-161, 2018.

THE ANNALS OF “DUNAREA DE JOS” UNIVERSITY OF GALATI
FASCICLE IX. METALLURGY AND MATERIALS SCIENCE
Nº. 1 - 2023, ISSN 2668-4748; e-ISSN 2668-4756
Article DOI: https://doi.org/10.35219/mms.2023.1.05

CUSTOM PROSTHETIC FINGER DEVICE USING 3D PRINTABLE PA11 CF POWDER

Gean-Carlos Nicholas DUMITRESCU[1], Patricia Isabela BRAILEANU[2*]
[1]University Politehnica of Bucharest, Faculty of Medical Engineering, Romania
[2]University Politehnica of Bucharest, Faculty of Mechanical Engineering and Mechatronics, Deparment of Machine Elements and Tribology, Romania
e-mail: gean.dumitrescu@stud.fim.upb.ro, patricia.braileanu@upb.ro*

ABSTRACT

This article presents a study on how to prototype a finger joint exoprosthesis using different CAD software and 3D printing techniques. The article describes the measurement of morpho-anatomical parameters, the creation of a 3D model based on these parameters, and the integration of an articulation mechanism into the patient's finger. This study also outlines the process of producing the custom prosthesis prototype by using PA11 CF material, which has applications in various fields including medicine. The prosthesis was then introduced to Sinterit Studio where a G-code was generated and the layers that would be printed were visualized. This method provides insight into the process of creating a prototype using 3D printing technology and specific software applications.

KEYWORDS: custom finger prosthesis, additive manufacturing, SLS

1. Introduction

Prototyping a finger joint prosthesis can be achieved through several methods, such as measuring the morpho-anatomical parameters of the index finger and creating a 3D model based on these parameters, or 3D scanning of the patient's hands and applying a mirror CAD function to the healthy finger in order to create a symmetrical prosthesis model with an articulation mechanism that will be integrated into the patient’s finger [1].

Each 3D printing process is based on a computer-generated graphic model created by various CAD (Computer Aided Design) applications. The graphics generated in CAD are exported as a mesh, with the most common format being STL (Standard Tesselation Language), which transforms the CAD model into a triangular representation. The mesh is introduced into a slicing software (e.g., Ultimaker Cura, Sinterit Studio) where the position and the number of pieces is established. In this slicer, the introduced model is divided into individual layers, each representing a 3D printing process.

To create the exoprosthesis, a mechanism consisting of regular bodies and the appearance of an integrated human finger is required, which presents irregular geometry. Since each CAD software has limitations in terms of tools that create easier geometry, we used the following CAD software:

a. *Blender* – is an open-source application for 3D creation, modelling, manipulation, simulation, animation, and rendering. Blender allows the modeling of polygonal meshes and uses vertices (points in 3D space) which are connected by lines. In this software, we can add vertices or modify their positions in the 3D space using specific tools, and we can edit the generated graphics' faces or geometry in any desired form.

b. *Autodesk Inventor Professional 2022* – is a CAD software that provides a range of tools for 3D modeling. This software allows the user to create the 3D body, reducing the risk of incorrect data transfer if the user wants to transform the model in a 2D drawing. Inventor is known for creating mechanisms and parts in the technical field, being able to create well-defined parts based on values or complex mathematical equations.

c. *Fusion 360* – is a software offered by Autodesk also used in 3D modeling, CAD, CAM, CAE, and a PCB platform for product design and manufacturing. This software is similar to Inventor but allows faster and easier 3D modeling. The user can design without the need to create a sketch, cut, or create an object. The list of tools in Fusion 360 allows us to modify the dimensions of faces and bodies in real-time, and we can also modify meshes, metal, and

THE ANNALS OF "DUNAREA DE JOS" UNIVERSITY OF GALATI
FASCICLE IX. METALLURGY AND MATERIALS SCIENCE
N°. 1 - 2023, ISSN 2668-4748; e-ISSN 2668-4756
Article DOI: https://doi.org/10.35219/mms.2023.1.05

plastic sheets. In addition, it also provides verification, testing, and FEA simulation.

d. *3D Builder* – Offered by Microsoft, is a software that allows the creation and modification of 3D files in formats such as 3MF, STL, OBJ, and PLY. It comes loaded with a wide range of 3D tools that are easy to use.

2. Experimental measurements and customized prosthesis modeling

For measuring the parameters, we used a 3D scan of a normal-sized hand from *Digital Reality Lab's* website, which we imported into Blender.

Using the mirror function, we created the second hand. For the left hand, we amputated the distal and medial phalanges of the second finger. We performed this amputation using the boolean function, creating a body with which we cut the mesh. The next step involved the "*measure*" function to measure the parameters necessary for the creation of the prosthesis. The measured parameters are presented in Table 1.

Using the data from the table below, we create a mechanism consisting of 3 parts in Autodesk Inventor Professional 2022. The mechanism is able to mimic the movements of a functional finger on a single axis. To create the parts, we started with simple 2D sketches that were transformed into 3D objects using the extrude function, along with fillet, sweep, revolve, and loft functions, which created 3 component parts that can form an articulating assembly similar to a human finger.

The 3 component parts have two circular holes that cross the parts (Figure 1); the holes have two roles: the first role is to extend the prosthesis, as an elastic band is introduced through this channel, allowing the prosthesis to return to its neutral position, where all angles between the parts are 180°. The second role is to flex the prosthesis, with the help of a high-resistance elastic wire attached to a bracelet on the patient's wrist, this can initiate the flexion of the distal phalanx, thus initiating the flexion of the entire prosthesis mechanism.

The images below show the 3 parts generated by Inventor Professional program and their assembly.

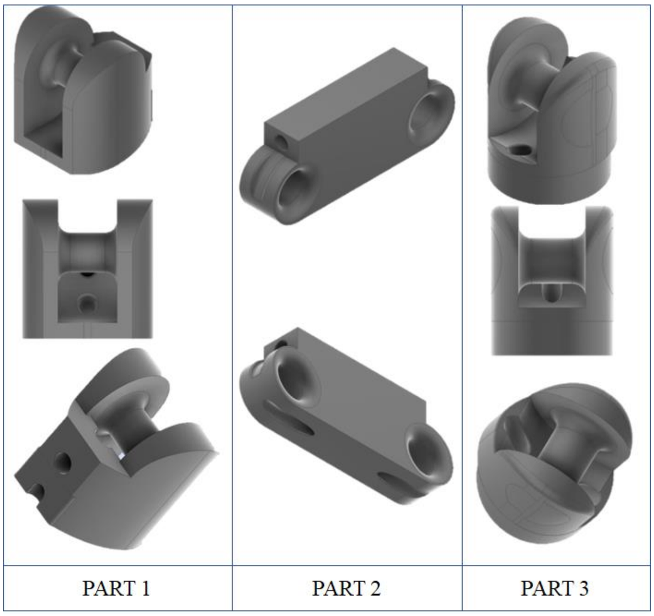

Fig. 1. *The component parts of the prosthesis assembly*

After creating the mechanism, we exported it in STL format and imported it into Blender, where the mirror function was used again to obtain the left hand. We cut off the finger that was initially amputated and used it to integrate the mechanism inside the finger. To integrate the mechanism inside the finger, we followed a few steps:

a. Positioning the assembly inside the finger, according to the measured parameters shown in Table 1.

b. Creating lines that follow the outline of the corresponding pieces of the distal-medial and proximal-median joints, and cutting the finger using the boolean function.

c. Sculpting inside the finger with the mechanism created in Inventor but for this step, it was necessary to fill the gaps in the parts to create a precise sculpting.

d. The final step involves placing the mechanism in the empty space inside the previously sculpted pieces. After placement, we used the "*Armature*" function, a tool that helps insert elements similar to a real skeleton, so we could articulate the component pieces precisely in the joint area where the mechanism axes are located.

Table 1. *Measurements of the parameters used to generate the prosthesis*

Parameter	Measured Area	Dimensions [mm]
Amputation top diameter	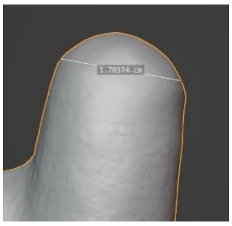	170
Amputation base diameter	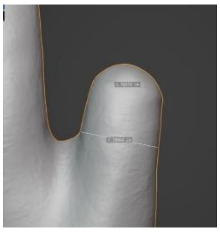	216
Amputation height - side	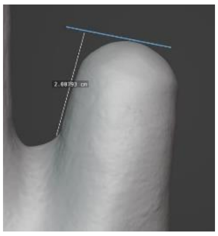	200
Amputation height - compared to the palm		220
Medial phalanx height		260
Distal phalanx height	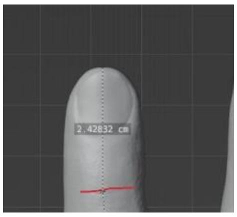	240

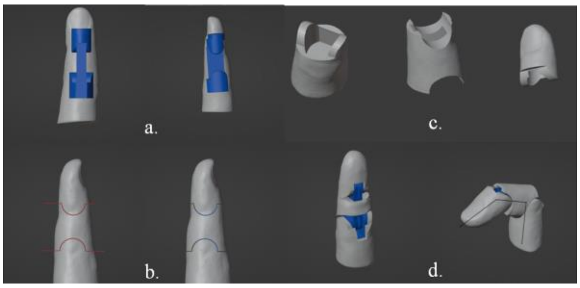

Fig. 2. *Custom finger prosthesis assembly. a. Fitting mechanism; b. Sectioning the finger; c. Creating space inside the finger for integrating the mechanism; d. Articulating the prototype using armatures*

After creating the prototype, we placed it on the hand with the amputated finger in order to make a comparison with the other hand and to observe how it fits on the mount, as shown in Figure 3.

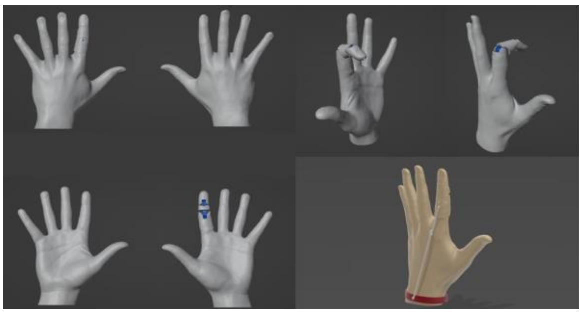

Fig. 3. *Presentation of the final virtual model of the custom prosthesis for the index finger*

3. Manufacturing method

The printing technology used for this prototype is SLS, with the help of the Sinterit Lisa Pro printer. Because is the only printing method through which mechanisms and parts containing multiple components can be printed without the need for supports and without gluing the parts together [2, 3]. Thus, assemblies can be directly printed with high precision. Compared to other printing techniques, it would have been necessary to create a prototype that would be assembled using separate components. The materials are divided into 3 categories:

a. Standard – the powders are excellent for prototyping and creating detailed objects with high resolutions.

b. Performance and special applications – these powders are used to create elements that require an extended life cycle, as well as high mechanical, chemical, and thermal resistance.

THE ANNALS OF "DUNAREA DE JOS" UNIVERSITY OF GALATI
FASCICLE IX. METALLURGY AND MATERIALS SCIENCE
Nº. 1 - 2023, ISSN 2668-4748; e-ISSN 2668-4756
Article DOI: https://doi.org/10.35219/mms.2023.1.05

c. Flexible – TPU and TPE powders are used to create flexible elements wherever flexibility with high mechanical properties is needed.

Among the available materials, we find: PA12 (rigid polyamide 12), PA11 (polyamide 11 with high mechanical strength and high elongation at break), PA11 ESD (polyamide 11, material from biological sources), PA11 CF (polyamide 11, the strongest and most versatile material available for SLS) [4]. Each material can be used by one or two printers in the range of those from Sinterit, with some materials only available for a specific type of printer. These materials find applications in the fields of production parts, automotive design, medical applications, tools, footwear, gaskets, and even aerospace parts.

Fig. 4. *3D printing results of the custom index finger prosthesis*

For the production of this model, we used PA11 CF (with carbon fiber) because it has applications in various fields, especially in medicine, where is used in medical equipment and prosthetics. Preparing the prototype for printing consisted of exporting it from Blender in STL format and importing the model in 3D Builder to check for imperfections that could cause printing errors, correcting the prototype, and then saving it in 3MF format. We introduced the prosthesis into Sinterit Studio, where we can position it according to the number of pieces we want to place or on which side we want the printing to start. The final 3D print results are shown in Figure 4.

4. Conclusions

The prototype developed in this study aimed to provide the patient with a method to produce a replacement for the amputated finger due to various pathological reasons and restore up to 70% of the movements of a healthy finger. This is an easy-to-create and printable prototype, which is parameterized and can be improved, such as by wrapping the prosthesis in a silicone material for better adhesion and a texture similar to that of the skin, making it moldable. Therefore, different shapes can be created that can be quite useful in the patient's activities. In the future, this prototype can be further developed, with the creation of a website where anyone can enter their measurements, and with the help of parametrization software, the prototype can be delivered with the appropriate dimensions, without the need for any CAD program intervention.

References

[1]. Kwon S. H., Wei-Kai Lao W., Ting-Wei Hsu A., Lee C. H., Hsu C. C., Huand J. J., Qiu S. S., Tilkorn S., Ting-Hsuan Tang E., Chuieng-Yi Lu J., Nai-Jen Chang T., *The Preferred Management of a Single-Digit Distal Phalanx Amputation*, J. Reconstr. Microsurg., vol. 36, no. 4, p. 301-310, 2020.

[2]. Su A., Al'Aref S. J., *History of 3D printing*, Elsevier Inc., 2018.

[3]. ***, *Introducing the 'Knick Finger' • 3D Printed Partial Finger Replacement Device–Enabling the Future*, https://enablingthefuture.org/2016/05/02/knickfinger/, accessed: Jun. 24, 2022.

[4]. Blanco I., *The use of composite materials in 3D printing*, J. Compos. Sci., vol. 4, no. 2, doi: 10.3390/jcs4020042, 2020.

[5]. Dumitrescu G. C. N., *Studii privind optimizarea exoprotezelor articulare ale degetului-index utilizând parametri morfo-anatomici*, Bachelor Thesis, 2022.

THE ANNALS OF “DUNAREA DE JOS” UNIVERSITY OF GALATI
FASCICLE IX. METALLURGY AND MATERIALS SCIENCE
Nº. 1 - 2023, ISSN 2668-4748; e-ISSN 2668-4756
Article DOI: https://doi.org/10.35219/mms.2023.1.06

TOPOLOGICAL OPTIMIZATION USING NEURONAL ALGORITHM

Gabriel PROCOPENCO, Florin-Bogdan MARIN, Mihaela MARIN
“Dunarea de Jos” University of Galati, Romania
e-mail: flmarin@ugal.ro, mihaela.marin@ugal.ro

ABSTRACT

Topological optimization is a type of structural optimization that provides conceptual design for lighter structures. The aim of this method is to maximize system performance for a given set of loads, boundary conditions, and constraints. This method is based on element analysis finished assembly. The design of a lightweight robot is a key point since the weight of the robot is directly proportional to the load capacity of the robot and its motor power. The structural design is iterated in a loop until function convergence achieves the objectives and the satisfying constraints.

KEYWORDS: topology optimization, robot, neuronal algorithm

1. Introduction

Nowadays 3D printing technology allows the manufacturing of complex volumes, imitating structures from nature [1, 2]. Topology optimization is a process in which the shape of a part is optimized based on specific design specifications, limited conditions, and loads, while the design remains structurally intact [4-6]. A practical approach to topology optimization is an analysis of finite elements to evaluate the performance of a shape, such as using an equivalent of von Misses stresses to determine the stresses on a shape. The next step, based on the analysis of the finite elements, is to execute or optimize the topology, to minimize the mass, and maximize the performance according to imposed conditions [7-12]. Topology optimization is very useful because it can build complex 2D or 3D shapes in a design space. However, it can give rise to problematic issues in the stage of manufacturing, such as the difficulties of manufacturing certain complex shapes which can be manufactured only using 3D printing technology. In 3D printing technology removing structural supports is an important issue. The resulting geometry for a typical topology optimization algorithm must be modified to match the capabilities of the manufacturing process [13, 14]. Additive manufacturing can be used to fabricate very complex geometries with a relatively small additional cost [15, 16]. Additive manufacturing is the most preferred process of manufacturing for shapes that have been designed through topology optimization. Topology optimization of a part for fabrication might produce an organic shape that is inspired by nature. However, solutions offered by some commercial topology optimization software must be post-processed so that the limited object fits the manufacturing process without unnecessary stress concentrations [17-21]. An important aspect of topology optimization is the selection of the mesh size. A fine mesh will provide a design more detailed but takes longer to run due to finite element analysis. A coarse mesh may not have the most optimal shape. Therefore, the mesh size should be selected with attention to balance these two aspects. The knowledge of 3D modeling is essential to the design process. The starting geometry (design space) for the topology optimization step influences the solutions that are determined. Selecting a design space that is too small can eliminate some of the possible solutions. However, the larger the design space, the better the computational cost of the topology optimization step is higher. For assembly, it is necessary to take into consideration how the system will be assembled (i.e. is it a simple feasible project). For loads and material properties, it is necessary to consider how large a selected load will be supported by the material. In addition, since the system will be 3D printed, it must be taken into account the part shrinkage. Topological optimization algorithm requires important computational resources. One way might be to use neural network algorithms to diminish computing time.

In this research, we aim to propose a neuronal algorithm in order to complete a proof-of-concept. Obviously, commercially available software is ready to solve the topological approach. Our proposed proof-of-concept approach shows the importance and

Nº. 1 - 2023, ISSN 2668-4748; e-ISSN 2668-4756
Article DOI: https://doi.org/10.35219/mms.2023.1.06

reliability of neural networks the topological optimization tasks.

2. Experimental procedure

The motor support was simulated as a whole, with loads given in the simulation for the weight-only transport box (Figure 1). The loads on each component were automatically calculated by the program for simulating static loads – Inventor Nastran. Network discretization, as it is shown in Figure 1 is dense enough to correlate a similar calculation with the real situation. In Figure 2 the part has been discretized with a much finer mean size to observe the time difference necessary for processing. Both cases brought the convergence of the calculation and similar results. The time of processing between the two cases was 30 minutes on a computer with about 10,000 points in PC Benchmark. Now that the part is set up, an FEA can be run to see how loads affect the shape, for example, to determine von Misses stresses. The simulation problem considers the loading in the 3D modeled assembly of the robot components of some static and dynamic loads. The static loads refer to a load of 5 Kg and the load is considered to act uniformly in the storage space for food transport, insecticide, and disinfectant substances. Generally, less material will increase the stress. However, if there are no stress concentrators in the design region and the maximum stress is within the safety factor, from the structural point of view, the part is feasible. If the stress exceeds the allowable stresses, the part must be modified until the stresses are within the acceptable range. The topology optimization results can be found below.

The neural network should learn from the training phase for 40 cases on different values of loading. The material considered in the simulation was PLA.

The procedural is considering several steps: 1. Firstly, 40 models with holes in the model at different dimensions are built manually and tested in Inventor Nastran for static loading. 2. The data for training is used to train the network. The input layer is consisting of 40 neurons representing the dimensions of the holes in the part and location. The output layer consists of 20 neurons representing the deformations in 20 points on the part. 3 resulted from each simulation. The testing data is represented by 10 scenarios with different loading forces. We used the Pytorch library to develop the neural network in the Spyder development environment. The network architecture considered 30 hidden layers. In order to test the result, Inventor Nastran was used and the performance factor is considered the mass reduction. The predictions outputted by the neural network show a 20% precision compared with the simulations in Inventor Nastran. Taking into account that few testing training data were used, the prediction might improve in case of using many testing.

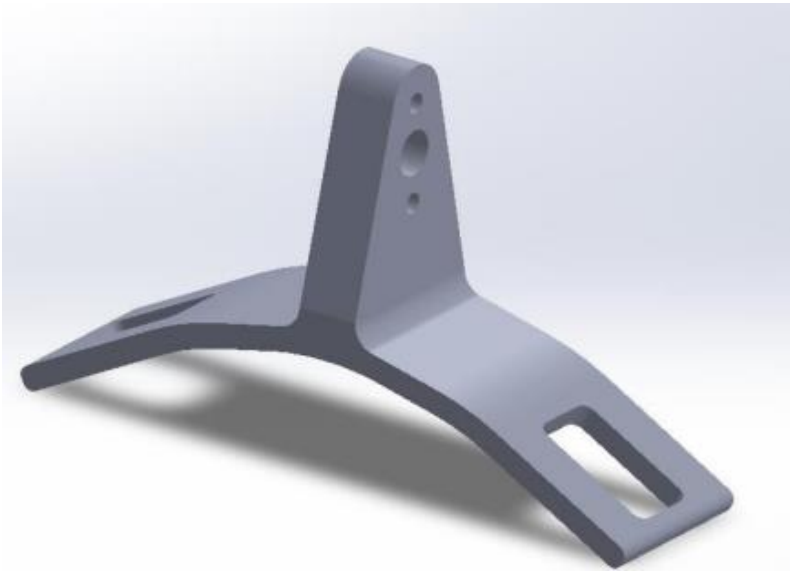

Fig. 1. *Un-optimized part*

THE ANNALS OF “DUNAREA DE JOS” UNIVERSITY OF GALATI
FASCICLE IX. METALLURGY AND MATERIALS SCIENCE
Nº. 1 - 2023, ISSN 2668-4748; e-ISSN 2668-4756
Article DOI: https://doi.org/10.35219/mms.2023.1.06

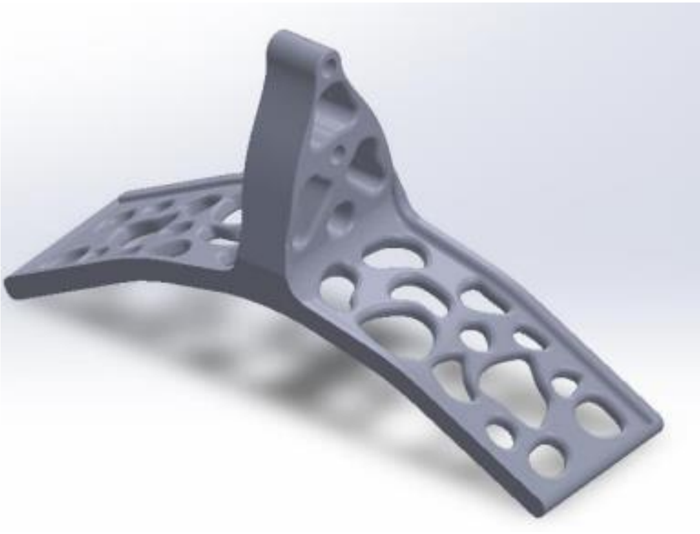

Fig. 2. *Topologically optimised part*

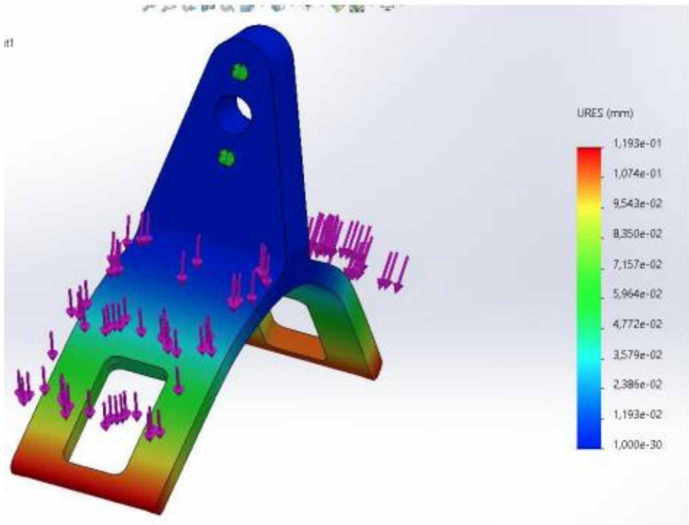

Fig. 3. *Deformation distribution for the support part*

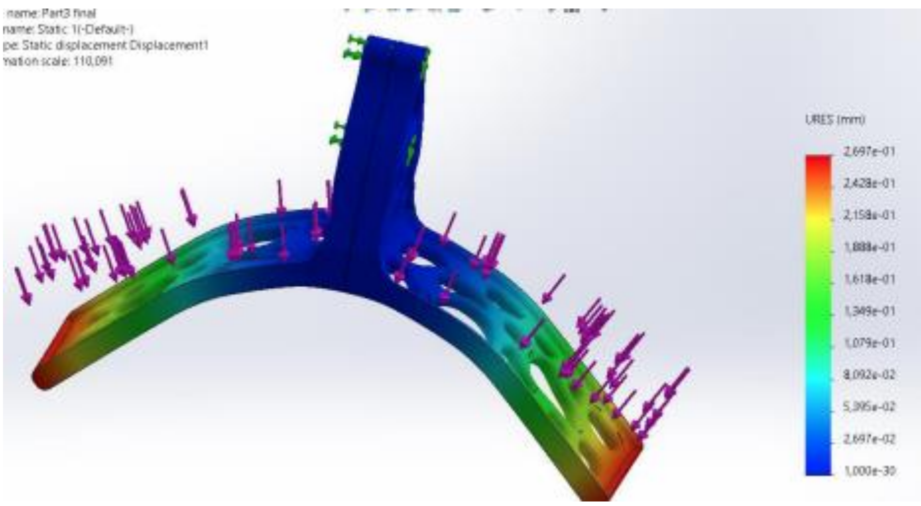

Fig. 4. *Deformation of a topological optimized part*

4. Conclusions

Topology optimization is a mathematical process that optimizes the appearance of a material based on specific design specifications, limited conditions, and loads while keeping the design structurally intact.

Topological optimization allows obtaining subassemblies that fulfil the conditions imposed but which require the use of a minimum amount of material.

3D modeling knowledge is required for the design process. The solutions that are determined are influenced by the starting geometry (design space) for the topology optimization step.

The deformation distribution shows that the part meets the conditions and can be considered for production.

Neural network algorithm provides promising results in topological optimization.

In this paper, the low precision of prediction outputted by the neural network is due to a small amount of training data.

References

[1] Syed T., Elias P. K., Amit B., Susmita B., Lisa O., Charitidis C., *Additive manufacturing: scientific and technological challenges, market uptake and opportunities*, Materials Today, vol. 1, p. 1-16, 2017.

[2]. Xian L. Z., Yen T. C., Ray M. R., Mattia D., Metcalfe D, Patterson A. D., *Perspective on 3D printing of separation membranes and comparison to related unconventional fabrication techniques*, Journal of Membrane Science.

[3]. Sha L., Lin A., Zhao X., Kuang S., *A topology optimization method of robot lightweight design based on the finite element model of assembly and its applications*, Science Progress, 103(3), 2020.

[4]. Zhu J., Chen X., *An engineering constraint method for continuum structural topology optimization*, Adv Mech Eng, 9: 1–6, 2017.

[5]. Cavazzuti M., Baldini A., Bertocchi E., *et al.*, *High performance automotive chassis design: a topology optimization based approach*, Struct Multidiscip Optim, 44, p. 45-56, 2011.

[6]. Duddeck F., Hunkeler S., Lozano P., *et al.*, *Topology optimization for crashworthiness of thin-walled structures under axial impact using hybrid cellular automata*, Struct Multidiscip Optim, 54, p. 415-428, 2016.

[7]. Wang X., Zhang D., Zhao C., *et al.*, *Optimal design of lightweight serial robots by integrating topology optimization and parametric system optimization*, Mechanism and Machine Theory, vol. 132, p. 48-65, 2019.

[8]. Long K., Yang X., Saeed N., *et al.*, *Topology optimization of transient problem with maximum dynamic response constraint using SOAR scheme*, Front. Mech. Eng., 16, p. 593-606, 2021.

[9]. Zargham S., Ward T. A., Ramli R., Badruddin I. A., *Topology optimization: a review for structural designs under vibration problems*, Struct. Multidiscip. Optim., 53, vol. 6., p. 1157-1177, 2016.

[10]. Kim B. J., Yun D. K., Lee S. H., Jang G. W., *Topology optimization of industrial robots for system-level stiffness maximization by using part-level metamodels*, Structural and multidisciplinary optimization, 54, p. 1061-1071, 2016.

[11]. Yunfei B., Ming C., Yongyao L., *Structural topology optimization for a robot upper arm based on SIMP method*, In Advances in Reconfigurable Mechanisms and Robots II, p. 725-733, Springer International Publishing, 2016.

[12]. Briot S., Goldsztejn A., *Topology optimization of industrial robots: Application to a five-bar mechanism*, Mechanism and Machine Theory, 120, p. 30-56, 2018.

[13]. Park G. J., *Technical overview of the equivalent static loads method for non-linear static response structural optimization*, Structural and Multidisciplinary Optimization, 43, p. 319-337, 2011.

[14]. Zuo K. T., Chen L. P., Zhang Y. Q., Yang J., *Study of key algorithms in topology optimization*, The International Journal of Advanced Manufacturing Technology, 32, p. 787-796, 2007.

[15]. Youn B. D., Choi K. K., *A new response surface methodology for reliability-based design optimization*, Computers & structures, 82(2-3), p. 241-256, 2004.

[16]. Stan S. D., Balan R., Maties V., *Multi-objective design optimization of mini parallel robots using genetic algorithms*, In 2007 IEEE International Symposium on Industrial Electronics, p. 2173-2178, IEEE, 2007.

[17]. Wang P., Huo X., Wang Z., *Topology design and kinematic optimization of cyclical 5-DoF parallel manipulator with proper constrained limb*, Advanced Robotics, 31(4), p. 204-219, 2017.

[18]. Liao Z. Y., Wang Y. J., Wang S. T., *Optimization design method of variable density lattice structure based on topology optimization*, Journal of Mechanical Engineering, 55(8), p. 65-72, 2019.

[19]. Yulin M., Xiaoming W., *A level set method for structural topology optimization and its applications*, Advances in Engineering Software, 35(7), p. 415-441, 2004.

[20]. Bendson M. P., *Generating optimal topologies in structural design using a homogenization method*, Computer Methods in Applied Mechanics and Engineering, 71, p. 197-224, 2008.

THE ANNALS OF “DUNAREA DE JOS” UNIVERSITY OF GALATI
FASCICLE IX. METALLURGY AND MATERIALS SCIENCE
N°. 1 - 2023, ISSN 2668-4748; e-ISSN 2668-4756
Article DOI: https://doi.org/10.35219/mms.2023.1.07

STUDIES AND RESEARCH ON SOIL ANALYSIS IN A DERELICT AREA, WHERE THERE WAS A LANDFILL

Beatrice Daniela TUDOR
“Dunarea de Jos” University of Galati, Romania
e-mail: beatrice.tudor@ugal.ro

ABSTRACT

In this paper, a study was made regarding the quality of the soil, from a disused area, where there was a garbage dump, which operated illegally. Soil samples were taken from different depths, namely 10, 20, and 30 cm deep, from 3 areas, covering the entire area where was the landfill. In the soil samples taken, the proportion of heavy metals and the pH were determined, thus being able to highlight how the quality of the soil was affected.

KEYWORDS: landfill, heavy metals, soil pollution

1. Introduction

Soil is represented by the surface layer of the earth's crust, made up of mineral particles, organic matter, water, air, and living organisms.

Soil develops and forms on the dry surface, that is, on the upper layer of rocks, on certain parts of the relief, under the action of environmental factors, which generate certain transformations of substances.

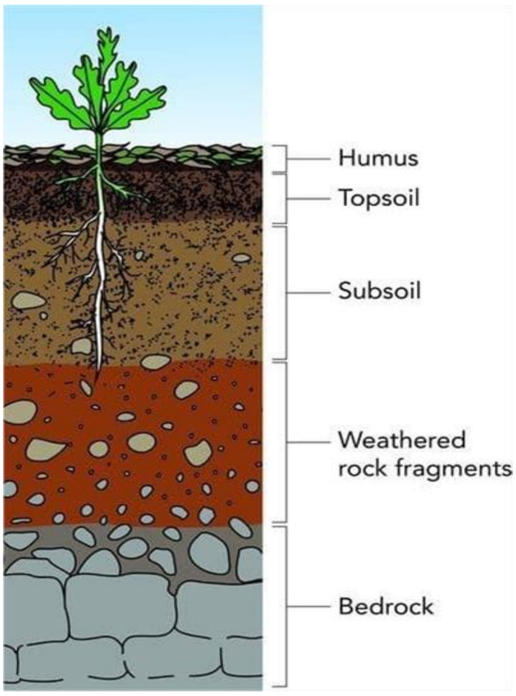

Fig. 1. *Soil horizons*

The process of soil formation is very long and consists of the interaction of several paedogenic factors such as mother-rock, living organisms (animals and microorganisms), climate, vegetation, relief, phreatic and surface water, and geological time [1, 3].

The soils are divided into layers, which depend on the depth. These are called horizons (Fig. 1).

Soil pollution is defined as the presence of toxic substances (pollutants or contaminants) in the soil, in concentrations sufficient to represent a risk to human health and the ecosystem.

2. Experimental research of soil quality

2.1. Establishment of soil analysis areas and research indicators

Soil samples were selected from a disused area, where there was a garbage dump, which operated illegally. Three soil samples were taken, from different depths (Fig. 2).

The investigated perimeters cover large areas, and the evaluation of the soil quality is the foundation of the examination of certain indicators, which measure the properties of the soil.

The criteria that were taken into account, when establishing the soil sampling points, had in mind:

- assessment of the soil situation in the contaminated territory;
- analysis of the elements present in each soil.

The samples were taken from different depths, respectively: 10 cm for sample 1; 20 cm for sample 2, and 30 cm for sample 3.

N°. 1 - 2023, ISSN 2668-4748; e-ISSN 2668-4756
Article DOI: https://doi.org/10.35219/mms.2023.1.07

From each sample, the pH and heavy metals were analysed. The following devices were used to determine the quality of the soil:

- X-ray fluorescence spectrometer (Innov-X Systems model) Fig. 3;
- the portable multiparameter HQ 40d (Fig. 4);
- analytical balance ALT 220-4NM;
- magnetic stirrer.

Fig. 2. *Landfill area*

Fig. 3. *X-ray fluorescence spectrometer*

Fig. 4. *Portable multiparameter HQ 40d*

2.2. Determination of heavy metals

Heavy metals have a potentially toxic effect on all living organisms, each of them, being dangerous if it exceeds a certain range of values. Thus, plants can accumulate heavy metals directly from the soil. Animals, especially herbivores, take them from the plants they feed on, or directly from the soil they graze on. People are exposed to the action of heavy metals, both through food and through the nature of work in the affected areas [2, 6].

The accumulation of heavy metals by living organisms will occur in different parts of the body, disrupting its proper functioning, at the enzymatic and cellular levels, leading to illness.

The reference values according to the MAPPM Order no. 756/1997 are presented in Table 1.

To determine the level of soil pollutant loading, soil samples were analysed, and the results were centralized in Table 2.

Table 1. *The reference values according to the MAPPM Order no. 756/1997*

Trace of chemical element	Normal values (mg/Kg)	Alert thresholds Types of use		Intervention thresholds Types of use	
		Sensitive	Less sensitive	Sensitive	Less sensitive
Ar	5	15	25	25	50
Co	15	30	100	50	250
Cr	30	100	300	300	600
Cu	20	100	250	200	500
Mn	900	1500	2000	2500	4000
Ni	20	75	200	150	500
Pb	20	50	250	100	1000
Zinc	100	300	700	600	1500

Table. 2. *The values of heavy metals determined in the soil samples from the landfill area*

Metal	Zone 1 Landfill			Zone 2 Landfill			Zone 3 Landfill		
	10 cm	20 cm	30 cm	10 cm	20 cm	30 cm	10 cm	20 cm	30 cm
TI	1808	1725	2146	2623	2219	1607	2710	3759	3767
Mn	348	367	308	295	352	250	165	471	390
Fe	10239	11209	11499	10165	10383	12597	9428	18059	15398
Ni					38				
Zn	193	52	38	98	256	544	41	67	130
Pb	43	12	10	25	27	110	13	18	21
Cu	28	37	48	34	30	34	43	71	68
Sr	88	36	41	173	75	321	37	102	143
Zr	90	125	104	132	76	174	102	275	296

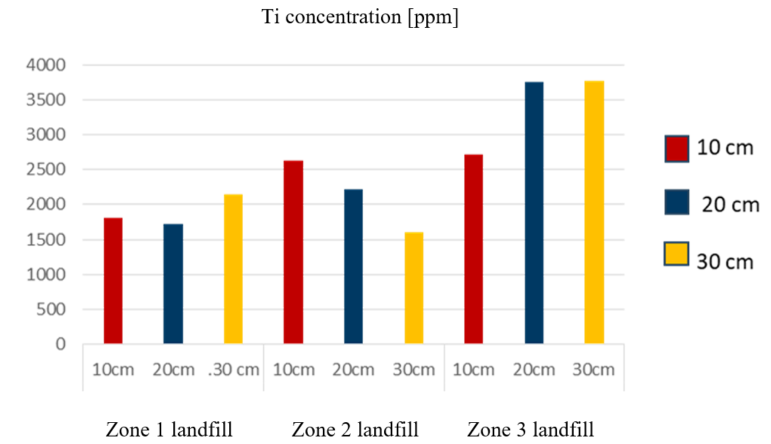

The determinations indicated heavy metals existing in the studied soil, respectively high values of Ti, which has an index of 3767, in zone 3 at a depth of 30 cm. A value that exceeds the allowed limit.

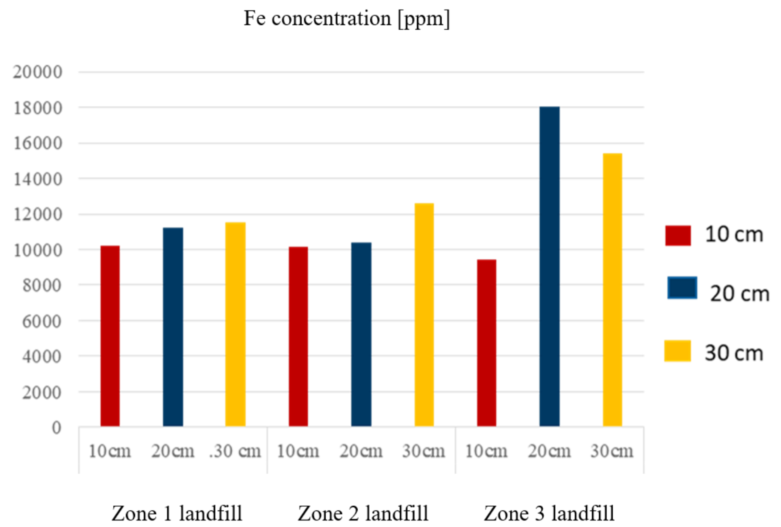

Fe has a very high concentration in all samples. The maximum value being reached, in the sample from the depth of 20 cm, from zone 3, with 15398 ppm.

THE ANNALS OF "DUNAREA DE JOS" UNIVERSITY OF GALATI
FASCICLE IX. METALLURGY AND MATERIALS SCIENCE
N°. 1 - 2023, ISSN 2668-4748; e-ISSN 2668-4756
Article DOI: https://doi.org/10.35219/mms.2023.1.07

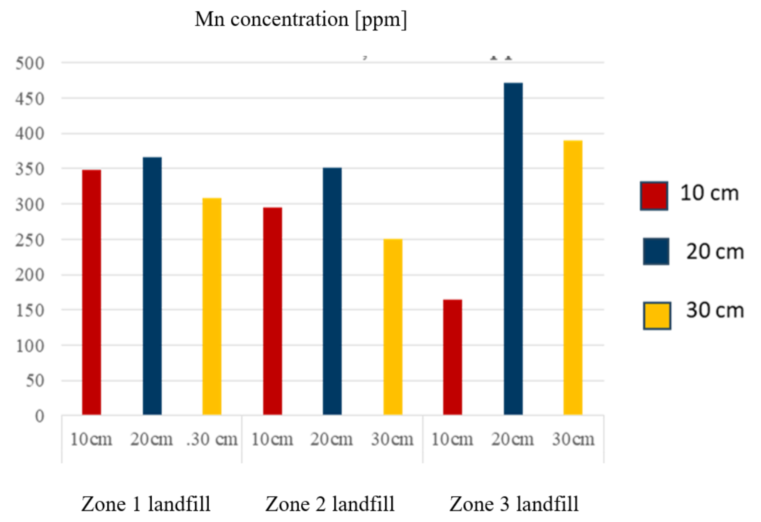

Mn shows a small exceedance of the limit values, for the sample from 20 cm from zone 3, and for the sample from 10 cm from the same zone, the values are within normal limits.

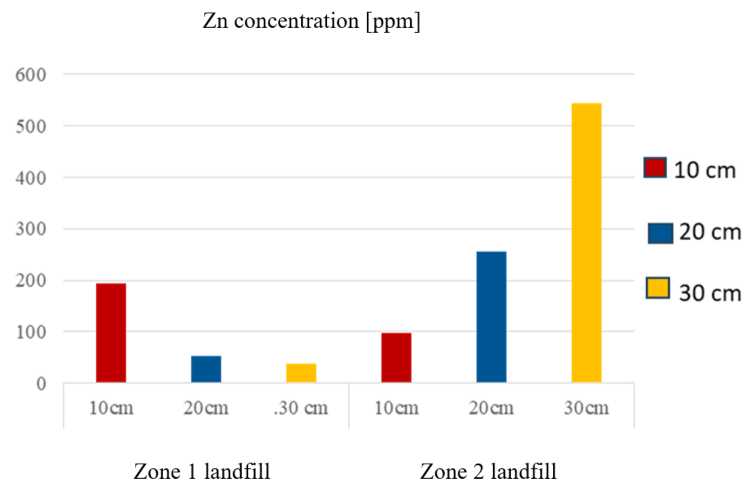

Zn shows values at the maximum limit in the samples taken from areas 1 and 2 and low values in area 3. Nevertheless, these values fall within the allowed limits.

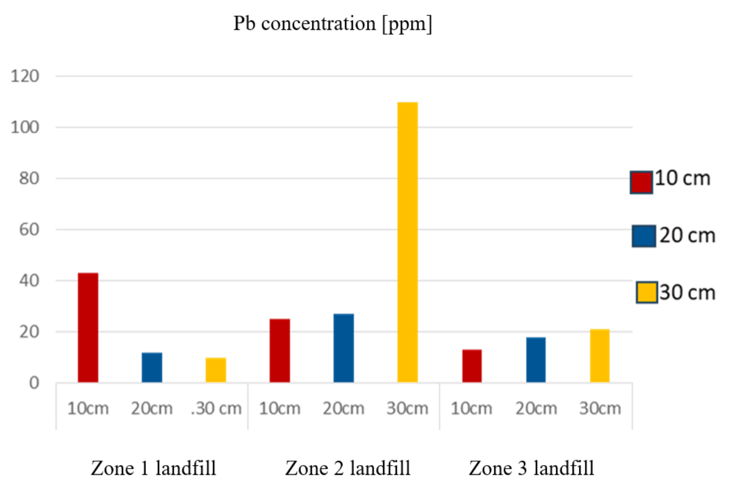

Nº. 1 - 2023, ISSN 2668-4748; e-ISSN 2668-4756
Article DOI: https://doi.org/10.35219/mms.2023.1.07

The concentration value of Pb is between 20 and 40 units in zones 1 and 3, and from the sample at 30 cm, from zone 2, the index exceeds the value of 100 ppm.

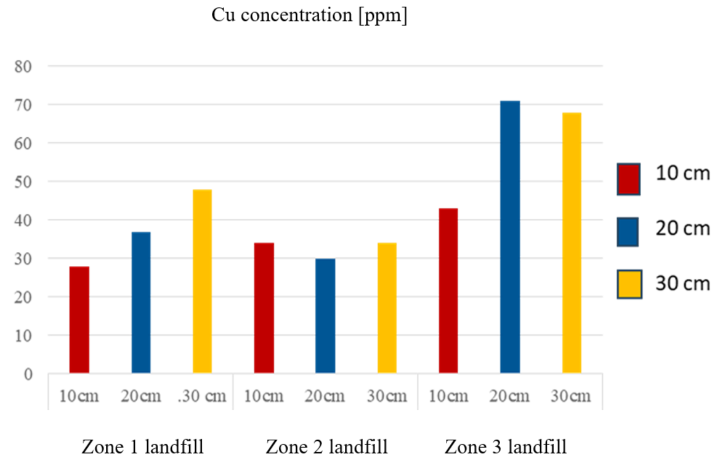

The X-ray spectrometer values for Cu increase in the samples from zone 3, from 20 and 30 cm, while for the other two zones, the values reach no more than 50 ppm.

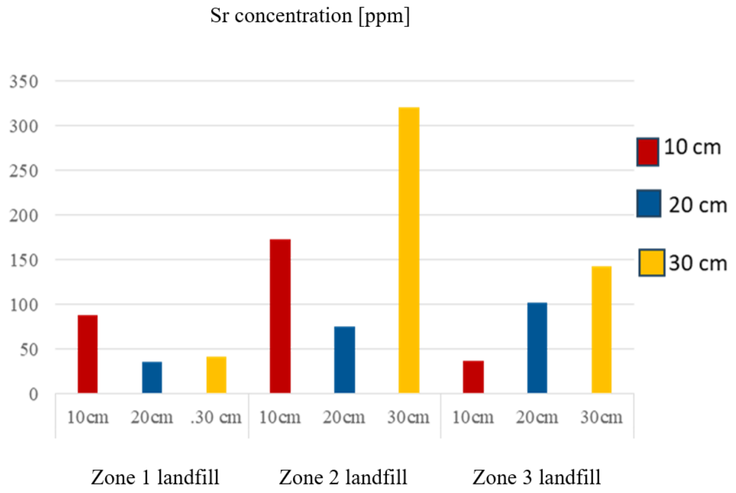

The determined concentration of Sr, following the analysis, indicates a certain increase in the sample from 30 cm from zone 2, and in zone 1 and 3 the values of the metal are between 20 and 200 units.

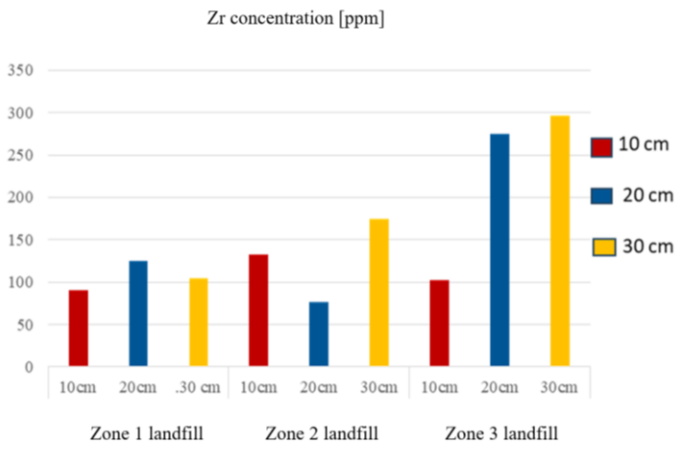

Another element found in all 9 samples is Zr, with a normal limit in zones 1 and 2, and an increase in value in zone 3, from 20 and 30 cm depth.

2.3. Determination of the pH of the soil samples taken from the former landfill

Soil pH refers to the concentration of positively charged hydrogen ions in soil moisture. The pH of the soil is measured on a scale from 0 to 14 (the lower the number, the more acidic the soil is), and this can affect the levels of essential nutrients in the soil. In soils, the pH value is between 3-3.5 and 9-9.5. Knowing the pH value is of great importance because it helps to characterize the salts, and to practice correct agricultural activity [4, 5].

The pH values determined for the soil samples from the 3 areas are centralized in Table 3.

Table 3. *pH values for the soil samples*

Zone 1	**pH**
10 cm	7.86
20 cm	7.16
30 cm	7.13
Zone 2	
10 cm	8.56
20 cm	8.37
30 cm	8.13
Zone 3	
10 cm	7.89
20 cm	7.56
30 cm	7.02

The pH analysis of the soil samples, from the area of the former landfill, shows us that the soil in areas 1 and 3 is weakly alkaline and in area 2 moderately alkaline. Alkaline soils, because they contain soda, can burn the roots of plants or cause the blocking of elements such as zinc, copper, and boron.

3. Conclusions

Soil pollution with heavy metals, from the area of the former landfill, is recognized today as a significant problem, representing a major risk to human health and the environment.

The disused landfill area was identified as one of the polluted areas, due to the long period of time in which the garbage was deposited, negatively affecting the environment and human health.

The concentration of heavy metals in the soil is significant, as a result of the high values of Zn, Fe, and Ti. Excessive amounts of heavy metals in the soil inhibit plant growth and negatively affect nitrogen fixation by microorganisms.

Heavy metal pollution is cumulative, which means that the pollutants accumulate slowly, being the result of permanent and long-term exposure of the soil to the action of these pollutants, without breaking down and without them being able to be removed.

The current state of soil pollution in the affected area is the result of the garbage storage activity carried out over the years.

The result of the analysis of the sampled soil highlights the fact that the studied area is polluted with Zn, Ti, Fe, Ni, and Mn. The analysis of the determinations made regarding Zn and Mn pollution highlights an alarming exceeding of the alert threshold.

The general conclusion indicates heavy metal pollution of the soil at the depth of 0-20 cm, requiring the undertaking of complex remedial activities.

The pH of the soil is within the limits of alkaline values. Alkaline soils, because they contain soda, can burn the roots of plants, or cause the blocking of elements such as zinc, copper, and boron.

References

[1]. Gavrilescu E., *Surse de poluare si agenti poluanti ai mediului*, Ed. Sitech, ISBN: 978-973-746-462-0, 2007.
[2]. Neag Gh., Culic Ana, Verraes G., *Polluted soils and waters. Treatment techniques*, Dacia Press, Cluj-Napoca, 2001.
[3]. Borlan Z., Hera Cr., *Metode de apreciere a stării de fertilitate a solului în vederea folosirii raţionale a îngrăşămintelor*, Ed. Ceres, Bucureşti, 1973.
[4]. Davidescu D., Davidescu Velicica, Lăcătuşu R., *Microelementele în agricultură*, Ed. Academiei RSR, Bucureşti, 1988.
[5]. Băjescu Irina, Chiriac Aurelia, *Distribuţia microelementelor în solurile din România*, Ed. Ceres, Bucureşti, 1984.
[6]. Bogaci Ruxandra, *Metode pentru aprecierea stării de asigurare a solurilor cu magneziu*, în "Metode, rapoarte, îndrumări" (I.C.P.A.), nr. 13, vol. 2, p. 240-245, 1981.

MANUSCRISELE, CĂRŢILE ŞI REVISTELE PENTRU SCHIMB, PRECUM ŞI ORICE CORESPONDENŢE SE VOR TRIMITE PE ADRESA:

MANUSCRIPTS, REVIEWS AND BOOKS FOR EXCHANGE COOPERATION, AS WELL AS ANY CORRESPONDANCE WILL BE MAILED TO:

LES MANUSCRIPTS, LES REVUES ET LES LIVRES POUR L'ECHANGE, TOUT AUSSI QUE LA CORRESPONDANCE SERONT ENVOYES A L'ADRESSE:

MANUSCKRIPTEN, ZIETSCHRITFTEN UND BUCHER FUR AUSTAUCH SOWIE DIE KORRESPONDENZ SID AN FOLGENDE ANSCHRIFT ZU SEDEN:

After the latest evaluation of the journals by the National Center for Science Policy and Scientometrics (**CENAPOSS**), in recognition of its quality and impact at national level, the journal will be included in the B^+ category, 215 code (http://cncsis.gov.ro/userfiles/file/CENAPOSS/Bplus_2011.pdf).

The journal is already indexed in:

DOAJ: https://doaj.org/

SCIPIO-RO: http://www.scipio.ro/web/182206

EBSCO: http://www.ebscohost.com/titleLists/a9h-journals.pdf

Google Academic: https://scholar.google.ro

Index Copernicus: https://journals.indexcopernicus.com

Crossref: https://search.crossref.org/

The papers published in this journal can be viewed on the website: http://www.gup.ugal.ro/ugaljournals/index.php/mms

Name and Address of Publisher:
Contact person: Prof. Dr. Eng. Elena MEREUȚĂ
Galati University Press - GUP
47 Domneasca St., 800008 - Galati, Romania
Phone: +40 336 130139
Fax: +40 236 461353
Email: gup@ugal.ro

Name and Address of Editor:
Ș. L. Dr. Eng. Marius BODOR
"Dunarea de Jos" University of Galati, Faculty of Engineering
111 Domneasca St., 800201 - Galati, Romania
Phone: +40 336 130208
Phone/Fax: +40 336 130283
Email: marius.bodor@ugal.ro

AFFILIATED WITH:

- THE ROMANIAN SOCIETY FOR METALLURGY
- THE ROMANIAN SOCIETY FOR CHEMISTRY
- THE ROMANIAN SOCIETY FOR BIOMATERIALS
- THE ROMANIAN TECHNICAL FOUNDRY SOCIETY
- THE MATERIALS INFORMATION SOCIETY
(ASM INTERNATIONAL)

Edited under the care of
the FACULTY OF ENGINEERING

Annual subscription (4 issues per year)

Fascicle DOI: https://doi.org/10.35219/mms

Volume DOI: https://doi.org/10.35219/mms.2023.1

Editing date: 15.03.2023
Number of issues: 200
Printed by Galati University Press (accredited by CNCSIS)
47 Domneasca Street, 800008, Galati, Romania